CHARACTERISTICS OF TORNADOES ASSOCIATED WITH LAND-FALLING GULF COAST TROPICAL CYCLONES

by

CORY L. RHODES

DR. JASON SENKBEIL, COMMITTEE CHAIR

DR. DAVID BROMMER

DR. P. GRADY DIXON

A THESIS

Submitted in partial fulfillment of the requirements

for the degree of Master of Science

in the Department of Geography

in the Graduate School of

The University of Alabama

TUSCALOOSA, ALABAMA

2012

ABSTRACT

Tropical cyclone tornadoes are brief and often unpredictable events that can produce fatalities and create considerable economic loss. Given these uncertainties, it is important to understand the characteristics and factors that contribute to tornado formation within tropical cyclones. This thesis analyzes this hazardous phenomenon, examining the relationships among tropical cyclone intensity, size, and tornado output. Furthermore, the influences of synoptic and dynamic parameters on tornado output near the time of tornado formation were assessed among two phases of a tropical cyclone's life cycle; those among hurricanes and tropical storms, termed tropical cyclone tornadoes (TCT), and those among tropical depressions and remnant lows, termed tropical low tornadoes (TLT). Results show that tornado output is affected by tropical cyclone intensity, and to a lesser extent size, with those classified as large in size and 'major' in intensity producing a greater amount of tornadoes. Increased values of storm relative helicity are dominant for the TCT environment while CAPE remains the driving force for TLT storms.

ACKNOWLEDGMENTS

I would like to thank my advisor and committee chair, Dr. Jason Senkbeil, and fellow committee members Dr. David Brommer and Dr. P. Grady Dixon for their encouragement, guidance and tremendous support throughout the entire thesis process. I would also like to show my gratitude towards those who graciously edited my thesis and provided helpful feedback. Lastly, I would like to thank my family, friends, and fellow colleagues for their constant support and encouragement during this time. This process would not have been possible without all of you.

CONTENTS

LIST OF TABLES

LIST OF FIGURES

1. Introduction

The Saffir-Simpson Hurricane Scale (SSHS, hereby referred to as SS) classifies tropical cyclones (TCs) as any storm with sustained wind fields of at least 38mph (17.0 m s^{-1}) which includes hurricanes, tropical storms, and tropical depressions (National Oceanic Atmospheric Administration 2012) (Table 1). Tropical cyclones are common during the months of May-November along the Gulf and Atlantic coastlines of the United States. Within these months, preparedness and continued alert are advised for residents, particularly within the vicinity of an approaching storm.

Table 1: Saffir-Simpson Hurricane Scale (revised 2012)

Classification	**Maximum Sustained Winds mph (knots)**
Tropical Depression	0-38 (0-34)
Tropical Storm	39-73 (35-63)
Category 1	74-95 (64-82)
Category 2	96-110 (83-95)
Category 3	111-129 (96-112)
Category 4	130-156 (113-136)
Category 5	>157 (≥137)

Land-falling TCs are accompanied by many well-known hazards, including coastal and inland flooding, wind damage, and storm surge. Eighty-two percent of TC-related casualties from 1970-1999 were attributed to flooding (primarily freshwater) from tropical cyclones (Rappaport 2000). The aftermath of Hurricane Camille (1969), for example, resulted in extensive coastal and inland flooding with damages totaling over $900,000 (Pielke et al 1999; Rappaport 2000). Rappaport (2000) found that only 12 percent of fatalities resulted from damaging winds. Hurricane Andrew (1992), for example, caused a reported $15 billion in structural damage as a result of wind during its multiple landfalls (Rappaport 1993), totaling 23 deaths during its paths through Florida and Louisiana, with 2 fatalities directly related to tornadoes (Rappaport 2000; Blake et al 2011). Storm surge, while primarily confined to coastal regions, is responsible for costly damages within land-falling tropical systems. Storm surge from Hurricane Katrina (2005) resulted in an estimated $75 billion in damages in New Orleans and along the Mississippi Gulf Coast (NHC 2012).

An often overlooked hazard that is a primary component of many land-falling TCs is that of embedded tornadoes, which, like the well-known hazards listed above, have the ability to destroy property, claim lives, and account for millions of dollars in damage. In its most general form, most tornadoes occur within TCs as a result of a sharp gradient in wind shear, brought on by the transition from water to land as a TC makes landfall (Moore and Dixon 2011). The majority of land-falling hurricanes are capable of producing tornadoes while approximately half of all tropical storms exhibit an environment that is favorable for tornado production (Gentry 1983). Tropical cyclone tornadoes can develop before, during and after tropical cyclone landfall.

A factor among TC tornadoes which surpasses all other associated hazards is the variability in timing and output (Hill, Malkin and Schulz 1966; Novlan and Gray 1974; Gentry 1983;

McCaul 1991; Schultz and Cecil 2009; Moore and Dixon 2011). Furthermore, tropical cyclone tornadoes can occur in both coastal and inland regions, which increases difficulty in forecasting and detection, and predicting economic loss and fatalities. It has been well-documented that tornadoes associated with land-falling TCs can occur well outside the envelope of known gale force winds (Pearson and Sadowski 1965; Hill, Malkin, and Schulz 1966; Orton 1970) where tornado awareness is lower. This increases risk to residents beyond the TC path (Weiss 1985; McCaul 1991; Spratt et al 1997).

Tropical cyclone tornadoes have contributed to approximately 4% of all TC-related fatalities (Rappaport 2000) and account for $1.4 billion in damages since 1950 (Schultz and Cecil 2009). Hurricane Beulah (1967), which spawned approximately 115 tornadoes during its lifetime, accounted for 5 fatalities and over $1.9 million in tornado-related damages (Orton 1970). Moreover, Hurricane Ivan spawned 118 confirmed tornadoes in September 2004, including 18 F2 and 1 F3-ranked tornado. Of these, two F2 tornadoes produced in Florida accounted for over $5 million in damages alone (National Climatic Data Center 2004). Although tornadoes comprise a small percentage of the total hazards accompanying TCs, they remain a viable threat within any land-falling system. Forecasting, detection, and analysis are crucial components in keeping residents continually abreast of this hazard.

This thesis considers previously analyzed aspects of TC tornadoes, with a specific focus on their characteristics, along with unanalyzed facets that are an important addition to the forecasting and detection of tornadoes within TCs. Climatology has been a well-studied aspect of TC tornadoes (Malkin and Galway 1953; Pearson and Sadowski 1965; Smith 1965; Hill, Malkin and Schulz 1966; Novlan and Gray 1974; Gentry 1983; McCaul and Weisman, 1996; Curtis 2004; Verbout et al 2007; Schultz and Cecil 2009; Edwards et al 2010; Moore and Dixon

2011), with individual focus placed on particular aspects, such as temporal and spatial distribution, frequency and intensity variations, as well as outbreak potential. In addition to climatological analysis, dynamic processes primary to the formation and detection of tornadoes within TCs have been performed.

In relation to TC intensity and tornado output (Novlan and Gray 1974; Gentry 1983; Weiss 1985), only one known study suggests utilizing these parameters in relation to storm size (McCaul 1991). McCaul's (1991) analysis of tornado output based on storm size and intensity suggests that the quantity and intensity of tornadoes increases with both TC intensity and size, as shown in Hurricanes Audrey (1957), Carla (1961), Beulah (1967) and Allen (1980). McCaul further emphasizes the importance of this study, stating that an analysis employing these parameters would be beneficial to forecasters in the tornado detection process within land-falling tropical systems.

As with tornado output within given stages of a TCs lifecycle, however, study authors have carried out this objective utilizing dynamic parameters (McCaul and Weisman, 1995; Curtis 2004; Edwards et al 2010). Although beneficial from the operational standpoint, a synoptic perspective would provide additional in-depth understanding of the atmosphere in which tornado formation occurs. Furthermore, this outlook would provide insight that may better predict tornado quantity and location within a storm. Cohen (2010) utilized a synoptic-based analysis to assess tropical cyclones along the Gulf Coast that produced a large quantity of tornadoes during their respective lifecycles.

Two primary objectives are analyzed within this thesis:

- Analyze the relationships between TC size, TC intensity, and TC tornado output

- Determine factors contributing to output and intensity differences for tropical cyclone tornadoes (TCT) and tropical low tornadoes (TLT) within land-falling TCs

This thesis is broken down into four subsequent chapters. Literature discussing the discovery, distribution, forecasting and detection of TC tornadoes is assessed in Chapter 2. Chapter 3 describes the methodology and statistical testing used to accomplish the objectives listed above. The results of these methods are shown in Chapter 4. Conclusions are discussed in Chapter 5.

2. Literature Review

2.1 Tropical Cyclone Tornadoes

Although reporting of TC tornadoes has been documented as early as 1773 (Sadowski 1962), the steady recording and assessment of tornadoes within land-falling storms was not readily documented prior to 1955. Several factors can be attributed to the tripling of the number of reported tornadoes in literature after 1950; storm detection by the public and NWS meteorologists; precision in storm accuracy; and the installation of the WSR-88D radar assisting in detection of rotation within land-falling TCs (Smith 1965; Agee and Hendricks 2011). Error and uncertainty in tornado reports can still result, including duplicate tornado reports leading to overestimates in widely populated regions, as well as an undercount in rural locations or where evacuation orders are advised (Orton 1970; Verbout et al 2007; Edwards 2010; Moore and Dixon 2011).

Throughout the years, a variety of research has been published on many aspects of TC tornadoes, including multiple long and short-term climatologies regarding the location, detection, forecasting, and formation of TC tornadoes. Furthermore, analysis among individual storms has been performed, including the tornado outbreaks of Hurricanes Beulah (1967) and Ivan (2004).

2.1.1 Climatology

Numerous climatologies have been performed on tornadoes of tropical origin, with frequent updates throughout the years. The earliest climatology of TC tornadoes dates to 1953, in which a dataset spanning 141 years resulted in 24 documented tornadoes (Malkin and Galway 1953). Several short-term climatologies were performed to evaluate particular characteristics of TC tornadoes, with datasets spanning 10 years or less (Pearson and Sadowski 1965; Smith 1965; Hill, Malkin and Schulz 1966). Larger datasets have evaluated TC tornadoes based on region within a tropical cyclone (Verbout et al. 2007; Schultz and Cecil 2009) or assessed individual dynamics that cause tornadoes to occur (McCaul and Weisman 1996; Curtis 2004; Edwards et al 2010). Specific factors explained in TC tornado climatologies are examined in the following sections.

2.1.2 Spatial Distribution

a. Regional Distribution

A dominant focus within TC tornado climatology examines the regional distribution of tornadoes along the southern and eastern coastlines of the United States. It has been shown that Gulf Coast land-falling tropical systems have a greater probability of tornado occurrence than storms making landfall along the Atlantic Coast (Smith 1965; Hill, Malkin and Schulz 1966; Novlan and Gray 1974; Gentry 1983; McCaul 1991; Verbout et al 2007; Schultz and Cecil 2009; Moore and Dixon 2011). Likely reasons for increased TC tornado occurrence along the Gulf include the orientation of the right-front (northeast) quadrant of the tropical cyclone making landfall along the coast, as well as, the length of time it is positioned along

the coastline (Pearson and Sadowski 1965; Smith 1965; Verbout et al 2007). It has been known (Malkin and Galway 1953; Novlan and Gray 1974; Gentry 1983; McCaul 1991; Davies 2006; Edwards and Pietrycha 2006; Verbout et al 2007; Cohen 2010; Moore and Dixon 2011) that the right front quadrant is a region containing strong convection and vertical and horizontal wind shear, which are the primary ingredients necessary for tornado formation and potential outbreaks. In addition, onshore flow (Eastin and Link 2009) evident within this quadrant maximizes convergence and lift, spawning tornadoes (Hill, Malkin and Schulz 1966; Novlan and Gray 1974; Gentry 1983; McCaul 1991; Moore and Dixon 2011). Furthermore, storm recurvature after landfall plays a significant role in tornado output, which is discussed in further detail in Section 2.2 as well as within the Results chapter. Alternatively, Atlantic storms are likely to make landfall from a north-to-northwesterly direction with regards to coastline orientation, with the right-front quadrant remaining over open waters (Novlan and Gray 1974). With this orientation – either a direct landfall in the N-NW direction or skirting the coast before recurvature into the Atlantic – the probability of tornadoes is reduced (Hill, Malkin, and Schulz 1966; Gentry 1983; McCaul 1991; Verbout et al 2007).

In regards to tornado distribution, there have been many guidelines regarding the exact threshold of tornado occurrence associated with TCs. Climatologically, the greatest chances of tornado occurrence reside just before TC landfall and upwards to 200km inland (Smith 1965; Novlan and Gray 1974; Gentry 1983; McCaul 1991; Schultz and Cecil 2009). Many authors, such as Spratt et al (1997), Kimball and Mulekar (2004), and Moore and Dixon (2011), however, designate a 400km radius when assessing maximum tornado activity within a tropical cyclone. The threshold has also been extended as far as 650km (Belanger et al

2009) and 800km (McCaul 1991) from circulation. Figures 1 and 2 show the most recent renderings of TC tornado spatial distribution, with buffers set at 200km (Schultz and Cecil 2009; Moore and Dixon 2011).

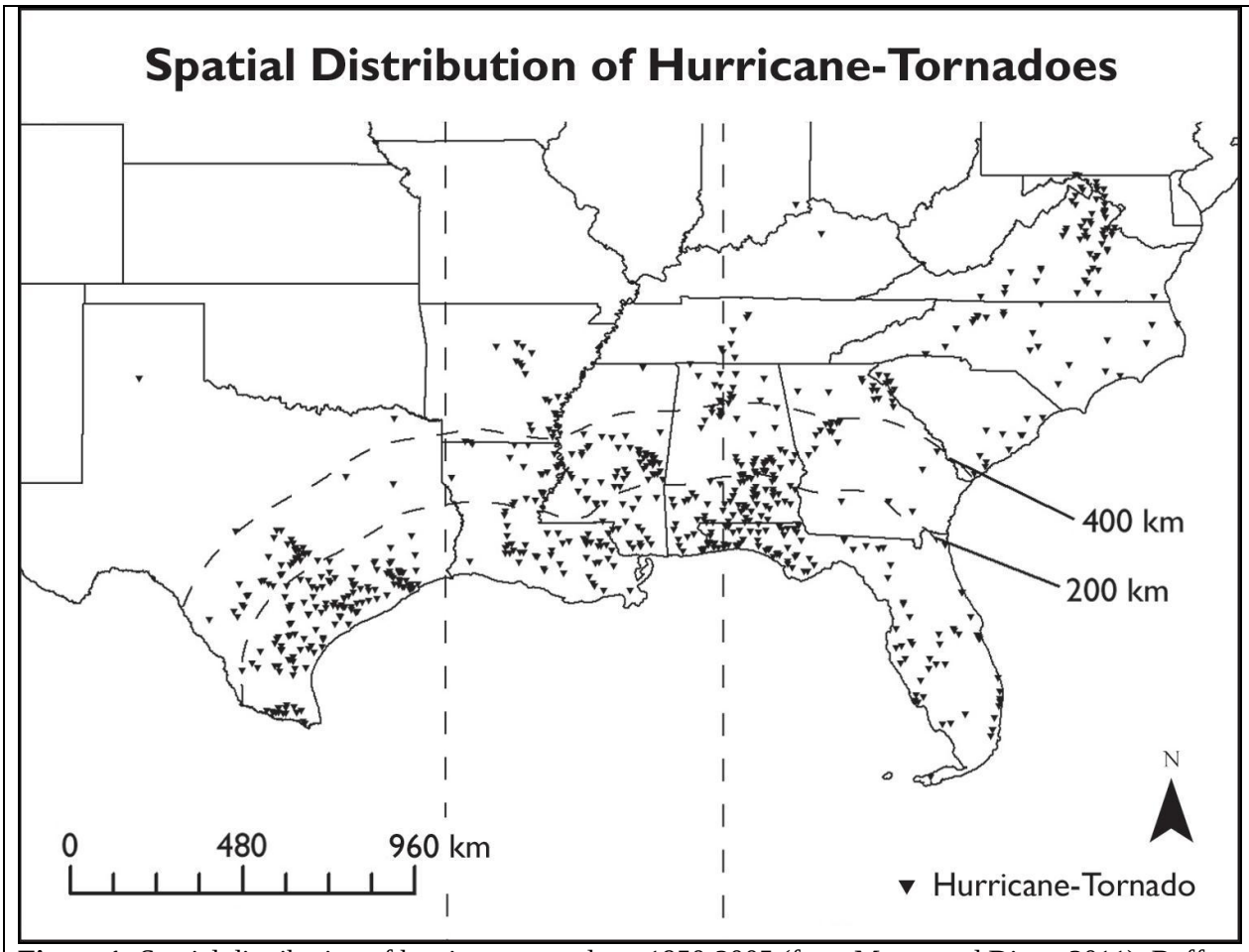

Figure 1: Spatial distribution of hurricane-tornadoes, 1950-2005 (from Moore and Dixon 2011). Buffers used to determine tornado output from coastline and set 200km apart. Dashed vertical lines represent longitude lines (at 94^0W and 87^0W, respectively) that segment the Gulf Coast into 3 separate regions.

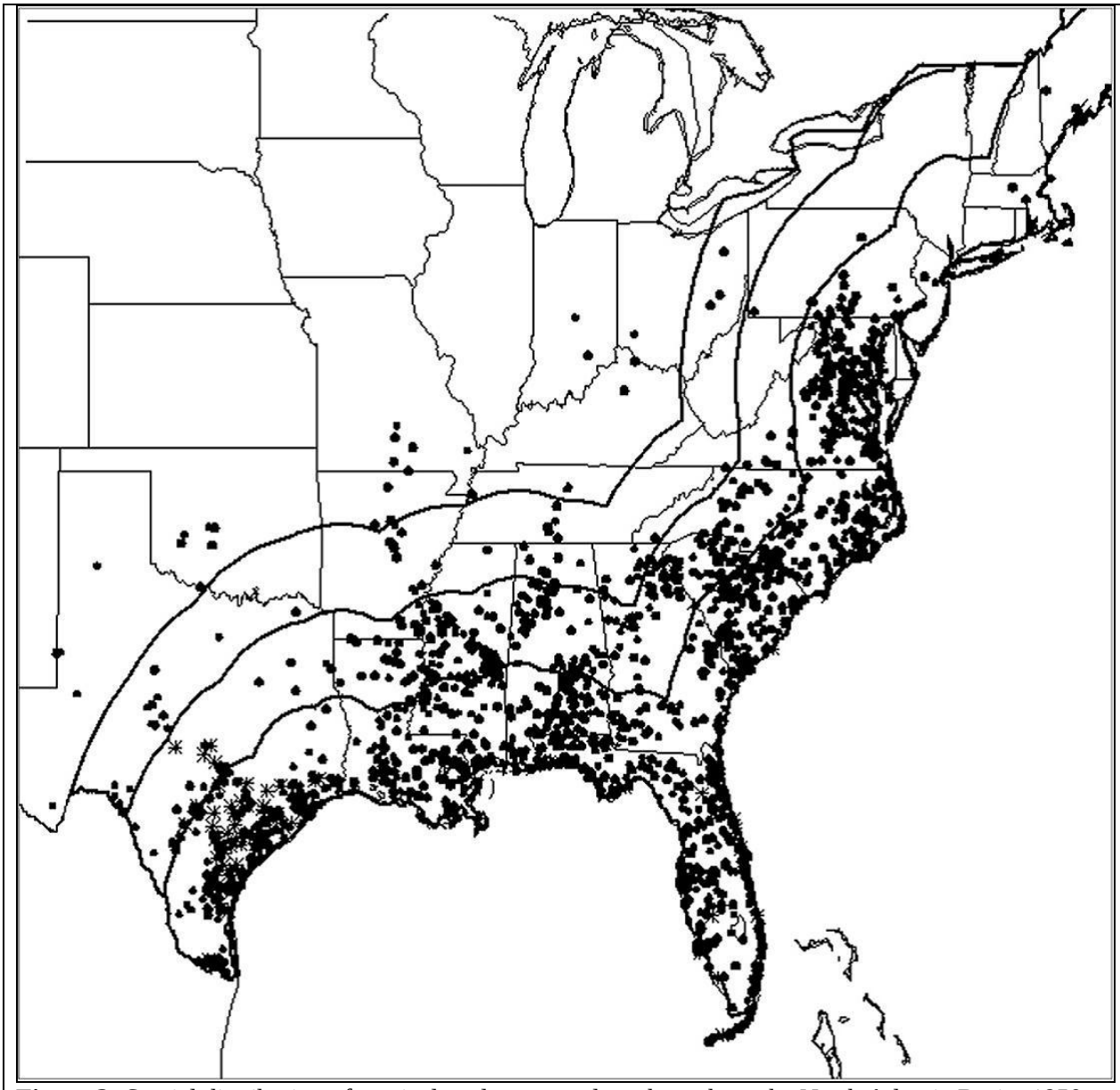

Figure 2: Spatial distribution of tropical cyclone tornadoes throughout the North Atlantic Basin, 1950-2007 (from Schultz and Cecil 2009). Buffers set at 200km beginning at the coastline.

The 200-400km radius employed in many studies is utilized as a result of the abovementioned water-to-land transition of tropical cyclones, increasing the likelihood of convergence within a region, thus aiding in uplift (Moore and Dixon 2011). Additionally, surface friction slows shallow surface winds while those further aloft (850mb) remain swift,

allowing low-level rotation to ensue (Gentry 1983; Curtis 2004) and tornadogenesis to occur more frequently closer to the coastline. Tropical cyclone tornadoes occurring outside the 200-400km threshold are usually the result of TC remnants that become engulfed into a synoptic or global-scale pattern (namely, mid-latitude troughs or the westerlies), or spawn as a result of low-level baroclinicity, such as an interaction with a frontal system (Schultz and Cecil 2009). The ingredients necessary to produce tornadoes are discussed in Section 2.2.

b. Tropical Cyclone Direction

Tornadoes associated with tropical cyclones typically occur in storms with a north or northeast directional heading (Smith 1965; Hill, Malkin and Schulz 1966; Novlan and Gray 1974; Moore and Dixon 2011). Many storms with this track tend to recurve post-landfall, spawning the majority of tornadoes during their lifetime. The recurving of the tropical cyclones predominantly results from three situations: 1) interaction with the westerlies, 2) engulfing of TC tornado remnants within a mid-latitude trough, and 3) the deepening of the low pressure system (TC) (Hill, Malkin and Schulz 1966; Verbout et al 2007; Schultz and Cecil 2009). Within these instances, the probability of a tornado outbreak is more likely.

Many authors take preference over a particular coordinate system when examining tornado location within tropical cyclones (Hill, Malkin and Schulz 1966; Orton 1970; Novlan and Gray 1974; Gentry 1983; Edwards 2010). With the majority of tornadoes spawning in the upper-right (northeast) sector of a tropical cyclone, it is of importance to distinguish between the two systems, as they can alter tornado dispersal within given sectors (Edwards 2010). Cartesian positioning associates each TC tornado location relative to true north,

utilized by Edwards (2010) in an assessment of TC tornado records. In other words, a tornado's location is derived from a distinct point along a coordinate plane system. Storm heading associates tornado location in relation to the direction of the tropical system. McCaul (1991) utilized storm heading in a climatology of environmental factors associated with TC tornadoes. The coordinate systems have been utilized interchangeably in the literature, which can cause misunderstandings about tornado location when a storm suddenly changes direction, as in the case of Hurricane Beulah (1967). As a result, preference for Cartesian rather than storm-relative directional heading is used (Edwards 2010).

c. Tornado Distribution Within Cyclone

In addition to areas of intense convection, tornadoes can be embedded within supercellular structures located in the inner eyewall or outer bands of a tropical cyclone within any quadrant (Hill, Malkin and Schulz 1966; Gentry 1983; Spratt et al 1997; Curtis 2004; Baker et al 2009; Schultz and Cecil 2009; Moore and Dixon 2011). It has been noted that the majority of tornadoes spawned from tropical systems occur outside the realm of known hurricane-force winds (Pearson and Sadowski 1965; Orton 1970; Edwards and Pietrycha 2010), predominantly embedded within outer rainbands that come ashore in advance or succession of the center of circulation. Tornadoes produced within outer bands result from shallow supercells that form offshore, spawning tornadoes once onshore as a result of surface friction (Eastin and Link 2009; Schultz and Cecil 2009).

Inner rainband tornadoes, encompassing approximately 20% of all TC tornadoes, are less frequent and most commonly result due to increased vertical wind shear and storm relative

helicity just before landfall (Gentry 1983; Schultz and Cecil 2009). Unlike outer rainband tornadoes, they are not necessarily associated with supercells but rather embedded within convective rain shields and areas in which cloud cover is present. Lack of diurnal heating inhibits buoyancy once onshore, further preventing tornadogenesis (Edwards et al 2010).

Early studies display biased opinions when documenting tornadoes within inner bands as detection and discrimination are difficult. Fujita classified inner band tornadoes within Hurricane Andrew (1992) after an intense survey to distinguish tornado damage from wind destruction (Hagemeyer and Hodanish 1997; Edwards 2010). Inner rainband tornado detection, therefore, can show a definite undercount as a result of Fujita's study.

2.1.3 Frequency

It has been shown that frequency of TC tornadoes is variable and storm specific (Belanger et al 2009; Moore and Dixon 2011). In Moore and Dixon's (2011) study, an increase in tornado frequency among land-falling hurricanes along the Gulf Coast was discovered, most notably in the 2004 and 2005 Atlantic hurricane seasons. The steady increase in hurricane-tornado frequency is likely attributable to advances in detection technology along with multiple reports of weak (F0) tornadoes. Furthermore, the recent spike in frequency can be attributed to the large outbreaks associated with Hurricanes Ivan (2004), Katrina (2005), and Rita (2005). Belanger et al (2009) showed that since 1995, TC size has increased, leading to a higher frequency of large tornado outbreaks, most notably in Gulf land-falling storms. Tornado frequency has also been shown to be dependent upon tropical cyclone stage (Hill, Malkin, and Schulz 1966; Novlan and Gray 1974). Tornadoes have a greater probability of occurrence when 1) a TC intensifies to

hurricane strength before landfall and 2) reaches any stage of deterioration while moving towards the northeast (Hill, Malkin, and Schulz 1966).

2.1.4 Intensity

Pertinent literature has shown a direct correlation between TC intensity and tornado output, stating the greater the TC intensity, the greater the tornadic output (and potential tornado outbreaks) within the storm (Smith 1965; Hill, Malkin, and Schulz 1966; Novlan and Gray 1974; Gentry 1983; Weiss 1985; McCaul 1991; Verbout et al 2007; Moore and Dixon 2011). Hill, Malkin, and Schulz (1966) note an increase of tornado development with intensifying storms, particularly before landfall. Moore and Dixon (2011) statistically analyzed this relationship and found that, based on Saffir-Simpson (SS) scale there is weak significance between hurricanes (namely, Category 1-4) and tornado output, with Category 3 hurricanes spawning the majority of tornadoes within the 55-year study.

2.1.5 Time of Day

While tornadoes within tropical cyclones can occur any time of the day, literature has repeatedly shown a diurnal distribution for TC tornadoes within land-falling systems (Novlan and Gray 1974; Gentry 1983; McCaul 1991; Schultz and Cecil 2009). Tornadoes can persist well before, during, and after landfall gradually decreasing approximately three days after the center of circulation has come ashore (Moore and Dixon 2011). The earliest known significant analysis in temporal distribution was performed by Novlan and Gray (1974), which resulted in

the majority of tornadoes within the study spawning at approximately 1700 Universal Time Coordinated (UTC). Through time, however, authors have noted that TC tornado dispersion likely peaks later during the day, most notably between the hours of 1800-2300 UTC (Gentry 1983; McCaul 1991) and 2000-2300 UTC (Schultz and Cecil 2009).

The tendency for tornadoes to occur within daytime hours results from a succession of dynamic factors, including increasing values of Convective Available Potential Energy (CAPE), strong vertical wind shear, and storm-relative helicity values (SRH), which, together, increase the energy-helicity index (EHI) and the probability for tornadoes (Davies-Jones 1984). Furthermore, the introduction of dry air intrusion into the storm aids in enhanced uplift and instability, which was first hypothesized by Latour and Bunting (1949). Conversely, individual authors of early studies such as Hill, Malkin and Schulz (1966) rejected a time distribution of TC tornadoes within the life cycle of a land-falling tropical system, stating that only a slight diurnal signal was present during the extratropical stage of a dissipating storm.

2.2 Tropical Cyclone Tornado Outbreaks

A range of explanations have been shown to constitute a tropical cyclone tornado outbreak (Smith 1965; McCaul 1991; Hagemeyer and Hodanish 1995; Hagemeyer 1997; Curtis 2004; Verbout et al 2007; Eastin and Link 2009; Edwards 2010; Moore and Dixon 2011). Bearing in mind spatial and temporal parameters, including advancements in tornado detection within recent years, there has been no clear threshold for the quantity of tornadoes needed for a TC to produce a tornado outbreak. Outbreaks within previous studies have been defined being as little as 4 tornadoes within a 4-hour period (Hagemeyer and Hodanish 1995) to as many as 20 within a 36-hour window of landfall (Curtis 2004). Furthermore, previous studies utilized various

classification schemes in order to assess these outbreaks in both number and severity. Although not deemed "outbreak", Hill, Malkin, and Schulz's (1966) study of tornadoes within land-falling TCs was assessed by classifying storms in terms of TC lifecycle. It was found that the majority of tornadoes developed within the hurricane stage of the tropical system. McCaul (1991) categorized TC tornadoes within the dataset based on three levels of outbreak: "minor" (8 or fewer tornadoes), "major" (greater than 8 tornadoes) and "severe" (greater than 24 tornadoes). Of this 39-year dataset, the majority of tornado outbreaks were classified as "major". Schultz and Cecil (2009) examined tornado outbreaks among two distinct regions to determine outbreaks within a given distance from the coastline. "Inner" or "core" region tornadoes occurred within 200km of the coast, while "outer" region tornadoes spawned beyond this threshold. It was determined that the area at greatest risk of a tornado outbreak occurred within 200km of the coast, most likely attributable to land-water transition. The next section is a discussion of the environmental conditions common for tornado formation (and tornado outbreaks) within land-falling TCs.

2.2.1 Environmental Conditions

a. Wind Shear

Early forecasters, such as Showalter and Fulks (1943) and Tepper (1950) have discussed wind shear as a possible essential environmental factor in the production of tornadoes. In association with hurricanes, Malkin and Galway (1953) noted a stronger occurrence of wind shear affecting the right-front quadrant of land-falling tropical systems, as illustrated in their assessment of tornadoes associated with Hurricane Able (1952). Willis (1969) and Novlan and Gray (1974) concluded that wind shear is paramount in the development of tornadoes

within storms. It was first noted that, upon landfall, winds aloft (4000-5000ft AGL) remained at speeds of approximately 55 knots while those near the surface slowed to approximately 15-20 knots (Willis 1969). Consequently, vertical wind shear increases just before TC landfall, aiding in the development of inner-region tornadoes (Schultz and Cecil 2009) as a hurricane begins to deteriorate once onshore (Novlan and Gray 1974).

Maddox (1973) hypothesized that the formation of localized vertical wind shear gradients was related to the development of a cold-core structure associated with a land-falling hurricane. Once inland, hurricanes lose their ability to generate a warm core as a result of being "cut off" from their primary energy source, filling at a rapid rate. This is later confirmed by Novlan and Gray (1974) as the predominant factor in tornadogenesis within storms. In addition, Gentry (1983) states that initial convergence, initiated by surface friction once the TC makes landfall, combined with increasing horizontal and vertical shear gradients results in core filling and temperature reduction of the TC. Once combined, the necessary ingredients for tornado formation are created.

b. Buoyancy

In relation to shear, buoyancy plays a large role in determining tornado occurrence within a land-falling TC, most notably in an environment conducive to supercellular development. To determine buoyancy within a TC, lifting parameters such as CAPE and Lifting Condensation Level (LCL) were examined (McCaul 1991; Schnieder and Sharp 2007). Low values of CAPE (<500 J/kg) have been consistently evident within the lower levels of some land-falling TCs, likely a result of deep saturation throughout. Schnieder and Sharp (2007) discuss the role LCL plays in increasing the probability of tornadoes within TCs. Lower

LCL, combined with smaller dewpoint depressions can weaken storm outflow, therefore increasing tornado probability. Edwards and Pietrycha (2010) further solidify this statement, asserting that lower LCL levels, higher low-level shear values, and enhanced storm-relative flow increase supercellular potential.

Additional components aiding in uplift include assessing existing buoyancy and rotation along baroclinic boundaries, most notably in the outer bands of a land-falling TC (Rao et al 2005; Verbout et al 2009). Edwards and Pietrycha (2010) assessed four classifications of tornado production along baroclinic boundaries within a TC environment, with variations in shear and/or buoyancy in four individual case studies. It was determined that tornadoes can form in both warm and cool sectors of a baroclinic boundary, dependent upon the limiting factors of shear and buoyancy. With a buoyant-limiting environment, shear is favorable on both sides, with buoyancy effective on the warm side of the zone. Shear-limiting environments show favorable tornado development along the cool side of the zone, provided buoyancy exists on both sides. Overlapping of both shear and buoyancy can occur along a baroclinic boundary, as noted with Hurricane Charley (2004), resulting in 13 reported tornadoes, akin to those that develop in the Great Plains (Edwards et al 2010). Tropical cyclones lacking in both shear and buoyancy on either side of the front remain weak in their supercell formation and tornado production, as shown with Hurricane Isabel (2003).

c. Storm Recurvature

Tropical cyclone recurvature has been a well-documented variable in association with tornado outbreaks (Smith 1965; Novlan and Gray 1974; Verbout et al 2007; Belanger et al 2009; Moore and Dixon 2011) and imperative in assessing variability among TCs (Verbout et al 2007; Belanger et al 2009). Storm recurvature results from the interaction of a weakening TC merging into a dynamic or synoptic-scale system, such as a mid-latitude trough base or the westerlies, where stronger and deeper shear is present (McCaul 1991; Hagemeyer 1998; Verbout et al 2007; Belanger et al 2009; Schultz and Cecil 2009). In general, storms with a north or northeast track are those primed for recurvature and potential tornado outbreak (Hill, Malkin and Schulz 1966; Moore and Dixon 2011). Recurvature among storms has been determined by evaluating the difference between average storm position 12 hours before landfall and 12 hours after the final advisory has been issued (Belanger et al 2009). Hurricanes Ivan (2004) and Rita (2005), for example, recurved once onshore, producing multiple tornado outbreaks during their lifetimes (National Climatic Data Center 2004, 2005).

d. Dry Air Intrusion

Dry air intrusion was hypothesized by Latour and Bunting (1949) in their radar assessment of a land-falling Florida hurricane (unnamed) during the 1949 Atlantic hurricane season. The authors noted "wave disturbances" in the northern semicircle of the hurricane, along which tornadoes occurred. It was theorized that once the hurricane approached land, an airmass with much cooler and drier conditions filtrated throughout the warm, moist tropical atmosphere, spawning tornadoes. Four years later, Malkin and Galway (1953)

hypothesized possible dry air intrusion as a factor in the Franconia, Virginia tornadoes that were spawned within the deteriorating stages of Hurricane Able in September of 1952.

In succeeding years, dry air intrusion became a primary focus in the study of TC tornadoes. Hill, Malkin and Schulz (1966) noted that storms with a northward heading leave their NW quadrant susceptible for cooler, drier air to penetrate the TC aloft, weakening the system and allowing a greater amount of low-level rotation to ensue. Dry air intrusion that penetrated storms was a result of increased low-level buoyancy. The availability of this was a result of limited cloud cover, which allowed for an increase in insolation (Schultz and Cecil 2009). Furthermore, dry air intrusion associated with outer rainbands sets the stage for strong, convective downdrafts in which baroclinic boundaries can occur in the lower levels, as described in part b (Hill, Malkin and Schulz 1966; Gentry 1983; McCaul 1991; Curtis 2004). These strong downdrafts create cold pools, or areas of cooler air, which can interact with low-level wind shear and increase values of CAPE, especially in the right-front quadrant, increasing the probability of a tornado outbreak (Curtis 2004; Baker et al 2009). The majority of these cold pools are much weaker than their synoptic counterparts, however, resulting in a greater amount of small-scale (F0, F1) tornadoes (McCaul and Weisman 1996).

2.2.2 Differences and Similarities to Synoptic Tornadoes

Tropical cyclone tornadoes show many similarities and differences in relation to tornadoes occurring in non-tropical environments associated with baroclinic zones. These types of tornadoes have been referred to as mid-latitude or Great Plains tornadoes (Hill, Malkin and Schulz 1966; McCaul 1987; McCaul and Weisman 1996; Spratt et al 1997; Edwards and Pietrycha 2006; Baker et al 2009; Eastin and Link 2009; Edwards 2010; Edwards et al 2010).

For the purposes of simplification, these mid-latitude or Great Plains tornadoes will be termed "synoptic" tornadoes in this thesis. To begin, TC tornadoes typically display shorter path lengths and narrow path widths (Hill, Malkin and Schulz 1966; Moore and Dixon 2011). Smith (1965) reports synoptic tornadoes are, on average, two times larger in both length and width than TC tornadoes. Concurrent with synoptic tornadoes, supercellular structures are known to develop within land-falling TC environments. Detection on radar, however, remains a difficult task in forecasting (Moore and Dixon 2011). Particular rotation signatures noted in synoptic tornadoes, such as a well-defined rotating updraft and notable hook echoes are virtually non-existent within TCs, resulting in brief if any lead times (Baker et al 2009). McCaul (1991) and Edwards (2010) note individual dynamics, including low-level buoyancy (such as CAPE and LCL) and shear values to be much smaller in TCs than synoptic tornadoes, likely attributable to the TCs saturated environment and cold core boundary layer, leading to a majority of weaker, short-lived tornadoes within TCs.

Similarities, however, can be seen among TCs and synoptic tornadoes. Particular tornadic components, including wall clouds, gust fronts, and strong straight-line winds are detected, as seen in those associated with Hurricane Danny (1985) (McCaul 1991). Furthermore, dynamically key ingredients, including variations in moisture, lift, instability, vertical wind shear, and baroclinic boundaries within TC environments mimic that of their synoptic counterparts, producing an environment similar to an "LP" or low precipitation supercell in certain cases (McCaul and Weisman 1996).

3. Data and Methods

3.1 Data Selection

This study encompasses not only hurricanes, which have been the primary focal point of many previous studies (Malkin and Galway 1953; Pearson and Sadowski 1965; Smith 1965; Novlan and Gray 1974; Gentry 1983; McCaul 1991; McCaul and Weisman 1996; Verbout et al 2007; Moore and Dixon 2011), but also tropical storms, as they can produce a large number of tornadoes during their life cycle. All TCs that made landfall along the states that border the Gulf of Mexico (Texas, Louisiana, Mississippi, Alabama, and the panhandle, western portion and southern tip of the Florida peninsula) are included in this thesis. The interior states of Georgia and Arkansas are also included, as many TCs recurve after landfall, and have commonly spawned tornadoes within these two states. Tropical cyclones that made landfall in Mexico within 250km of the TX border and spawned tornadoes were included in the dataset. A total of 95 TCs made landfall along the Gulf Coast during the 1950-2010 study period (61 hurricanes and 34 tropical storms), resulting in a total of 1194 tornadoes within the study area. All TCs that made landfall within the study area are displayed in Table 2. Within this dataset, 13 TCs either downgraded before landfall or intensified during their track; therefore, although listed by NHC assigned rating, these TCs will be referred to by their inland status in this study. In order to fully assess the objectives within the study, many data sources were used.

Table 2: List of all land-falling TCs in study area, 1950-2010, including landfall date, intensity, Saffir-Simpson category, and total tornado output.

Tropical Cyclone	Landfall Date	Intensity at Landfall (mph)	Saffir-Simpson Category (at Landfall)	Total Tornado Output
Tropical Storm Hazel	9-Oct-1953	70	TS	1
Hurricane Flossy	24-Sep-1956	75	1	3
Hurricane Audrey	27-Jun-1957	145	4	23
Tropical Storm Esther	18-Sep-1957	50	TS	1
Tropical Storm Arlene	30-May-1959	45	TS	1
Hurricane Debra	25-Jul-1959	85	1	2
Hurricane Judith	18-Oct-1959	50	TS	2
Tropical Storm #1	24-Jun-1960	45	TS	3
Hurricane Ethel	15-Sep-1960	70	TS	1
Tropical Storm Florence	23-Sep-1960	30	TD	1
Hurricane Carla	11-Sep-1961	145	4	21
Tropical Storm #1	6-Jun-1964	35	TD	3
Hurricane Hilda	3-Oct-1964	115	3	7
Hurricane Isbell	14-Oct-1964	125	3	9
Tropical Storm #1	15-Jun-1965	50	TS	2
Hurricane Betsy	10-Sep-1965	155	4	6
Hurricane Alma	9-Jun-1966	90	1	4
Hurricane Beulah	20-Sep-1967	160	5	117
Hurricane Abby	4-Jun-1968	65	TS	4
Tropical Storm Candy	24-Jun-1968	70	TS	7
Hurricane Gladys	19-Oct-1968	80	1	2
Hurricane Camille	17-Aug-1969	190	5	2
Tropical Storm Jenny	3-Oct-1969	40	TS	2
Tropical Storm Becky	22-Jul-1970	45	TS	2
Hurricane Celia	3-Aug-1970	125	3	8
Hurricane Fern	10-Sep-1971	70	TS	5
Hurricane Edith	16-Sep-1971	100	2	16
Hurricane Agnes	19-Jun-1972	75	1	17
Tropical Storm Delia*	5-Sep-1973	65	TS	5
Hurricane Carmen	8-Sep-1974	150	4	6
Hurricane Eloise	23-Sep-1975	125	3	5
Hurricane Babe	5-Sep-1977	75	1	13
Tropical Storm Debra	29-Aug-1978	60	TS	4
Hurricane Bob	11-Jul-1979	75	1	2
Tropical Storm Claudette	24-Jul-1979	50	TS	2
Hurricane Frederic	13-Sep-1979	135	4	10
Hurricane Allen	10-Aug-1980	115	3	34
Tropical Storm Danielle	6-Sep-1980	45	TS	5
Tropical Storm Chris	11-Sep-1982	65	TS	9
Hurricane Alicia	18-Aug-1983	115	3	22
Hurricane Bob	23-Jul-1985	45	TS	2
Hurricane Danny	15-Aug-1985	90	1	31
Hurricane Elena	2-Sep-1985	115	3	9
Hurricane Juan*	28-Oct-1985	85	1	13
Hurricane Bonnie	26-Jun-1986	85	1	5
Hurricane Florence	10-Sep-1988	80	1	4
Hurricane Gilbert	16-Sep-1988	135	4	39
Tropical Storm Keith	23-Nov-1988	65	TS	2
Tropical Storm Allison	26-Jun-1989	45	TS	9
Hurricane Chantal	1-Aug-1989	80	1	4
Hurricane Jerry	16-Oct-1989	85	1	7
Tropical Storm Marco	12-Oct-1990	35	TD	2
Hurricane Andrew	26-Aug-1992	140	4	48
Tropical Storm Beryl	16-Aug-1994	60	TS	2
Hurricane Gordon	16-Nov-1994	50	TS	5
Hurricane Allison	5-Jun-1995	70	TS	7
Tropical Storm Dean	31-Jul-1995	45	TS	2
Hurricane Erin	3-Aug-1995	75	1	5
Hurricane Opal	4-Oct-1995	125	3	19
Hurricane Danny	19-Jul-1997	75	1	2
Hurricane Earl	3-Sep-1998	80	1	9
Tropical Storm Frances	11-Sep-1998	50	TS	9
Tropical Storm Hermine	20-Sep-1998	45	TS	2
Hurricane Georges	28-Sep-1998	105	2	49
Hurricane Mitch	5-Nov-1998	60	TS	6
Hurricane Bret	23-Aug-1999	115	3	6
Tropical Storm Harvey	21-Sep-1999	60	TS	2
Hurricane Irene	15-Oct-1999	75	1	4
Hurricane Gordon	18-Sep-2000	70	TS	7
Tropical Storm Helene	22-Sep-2000	40	TS	10
Tropical Storm Allison*	5-Jun-2001	60	TS	15
Hurricane Gabrielle	14-Sep-2001	70	TS	19
Tropical Storm Fay	7-Sep-2002	60	TS	11
Tropical Storm Hannah	14-Sep-2002	60	TS	1
Hurricane Isidore	26-Sep-2002	65	TS	10
Hurricane Lili	3-Oct-2002	90	1	27
Tropical Storm Bill	30-Jun-2003	60	TS	15
Hurricane Claudette	15-Jul-2003	85	1	2
Tropical Storm Bonnie	12-Aug-2004	50	TS	6
Hurricane Charley	13-Aug-2004	145	4	17
Hurricane Ivan	16-Sep-2004	120	3	54
Tropical Storm Matthew	10-Oct-2004	45	TS	1
Hurricane Cindy	6-Jul-2005	75	1	28
Hurricane Dennis	10-Jul-2005	125	3	9
Hurricane Katrina	29-Aug-2005	145	4	49
Hurricane Rita	24-Sep-2005	115	3	104
Hurricane Wilma	24-Oct-2005	125	3	8
Tropical Storm Alberto	13-Jun-2006	50	TS	3
Tropical Storm Erin	16-Aug-2007	40	TS	2
Hurricane Humberto	13-Sep-2007	90	1	1
Hurricane Dolly	23-Jul-2008	85	1	5
Tropical Storm Fay*	19-Aug-2008	65	TS	34
Hurricane Gustav	1-Sep-2008	110	2	19
Hurricane Ike	13-Sep-2008	110	2	33
Tropical Storm Hermine	7-Sep-2010	65	TS	11

* denotes initial landfall

Sources: NCDC 2011; NHC 2011

3.2 Data Sources

a. National Climatic Data Center (NCDC)

All tornadoes that occurred during the Atlantic hurricane seasons of 1950-2010 were extracted from the National Climatic Data Center's (NCDC) Storm Events database. Information within this database includes the tornado's date and time of occurrence, approximate starting and (if available) ending coordinate locations, path length and width estimates, Fujita scale rating (if assigned), county of occurrence, including approximate damage and crop loss estimates, and fatalities, if applicable (NCDC 2011). An update to the database in 1992 adjusted time of occurrence to local standard time, specified location within street-level accuracy, and included meteorological and environmental descriptions as to the formation of the tornadoes that occurred.

All tornadoes within NCDC's Storm Events database were documented using the Fujita Scale (F-Scale) rating. The Fujita Scale was revised in 2007 to the Enhanced Fujita Scale (EF-Scale), adjusting wind parameters for each category (SPC 2012). The final three years of this dataset fall into the EF-Scale adjustment; however, NCDC has continued documenting tornadoes utilizing the Fujita Scale throughout the duration of this study period, allowing for a concurrent documentation of tornadoes. Therefore, the Fujita Scale is used throughout this thesis as the primary tornado rating system. The Fujita and Enhanced Fujita Scales, along with the Operational Scale utilized by the Storm Prediction Center (SPC) are displayed in Table 3 below.

Table 3: Fujita Scale and Derived Enhanced Fujita Scale, including scale for operational use.

FUJITA SCALE			DERIVED EF SCALE		OPERATIONAL EF SCALE	
F Number	**Fastest 1/4-mile (mph)**	**3 Second Gust (mph)**	**EF Number**	**3 Second Gust (mph)**	**EF Number**	**3 Second Gust (mph)**
0	40-72	45-78	0	65-85	0	65-85
1	73-112	79-117	1	86-109	1	86-110
2	113-157	118-161	2	110-137	2	111-135
3	158-207	162-209	3	138-167	3	136-165
4	208-260	210-261	4	168-199	4	166-200
5	261-318	262-317	5	200-234	5	Over 200

Source: SPC 2012

An additional database that examines tornadoes within a land-falling TC, entitled TCTOR (Tropical Cyclone TORnado) is also available. TCTOR was used within this thesis as a comparison to the NCDC database that was primarily used to obtain data for this thesis. The database was created in 2010 by Edwards as a reanalysis of NCDC's original database, assessing each land-falling TC to ensure accuracy and reduce redundancy in the documentation and analysis of tornadoes. Each observation was carefully analyzed and compared to surface and upper-air observations, radar, and satellite data to ensure its connectivity to a land-falling TC. This data, however, is archived from 1995-present; therefore, the information provided was used for comparison purposes to the Storm Events database for the years listed.

b. NOAA's Coastal Services Center Historical Hurricane Tracks

In order to associate these tornadoes with a Gulf land-falling TC, the National Oceanic and Atmospheric Administration's (NOAA) Coastal Services Center (CSC) Historical Hurricane Tracks database was used (CSC 2011) and available online

(http://csc.noaa.gov/hurricanes/#). This database employs an interactive GIS-based mapping approach, detailing the path of each TC from inception to dissipation, using color-coding to display intensity variations during the life cycle of the TC in shapefile format. In addition, the CSC provides detailed advisories at 6-hour intervals (00Z, 06Z, 12Z, and 18Z), recording the date and time (in GMT) of each advisory, latitudinal and longitudinal position of the storm, pressure (in millibars), maximum sustained winds (MSW) (in knots) and SS category at time of advisory, which is displayed in table and interactive graph format within the database. The SS category changes within each TC were monitored using this database in order to assign tornado output among two phases of a TC's life cycle generated by the author. Tornadoes that spawned during the TC's hurricane or tropical storm phase were listed as Tropical Cyclone Tornadoes (or TCT), while those which spawned during the tropical depression or remnant low phases were entitled Tropical Low Tornadoes, or TLT. The tornadoes extracted from NCDC's Storm Events database where then placed into one of these two groups based on TC intensity level when spawned.

c. National Hurricane Center HURricane DATabase (HURDAT), Best Track and Extended Best Track Datasets

The National Hurricane Center's (NHC) Hurricane Database (known as HURDAT), originally created in the 1960s under NASA's Space Program, was devised to better understand the track and forecast observations of land-falling TCs of the North Atlantic Basin in relation to space shuttle launches from Florida's Kennedy Space Center (Jarvinen et al 1984). The database primarily consisted of intensity variations among TCs within a 72-hour period. Amidst technological advances in succeeding years leading to numerous revisions, the current database includes a detailed account of each TC advisory, including 6-

hour observations of latitude, longitude, surface winds (1-minute sustained maximum), minimum sea-level pressure, and tropical status (tropical, subtropical, or extratropical, respectively) for each known land-falling TC dating back to 1851.

The Best Track dataset includes landfall information for each TC and is a reanalysis of the original HURDAT database. The update to the HURDAT database included clearing errors in documentation, utilizing new analysis techniques in order to correctly identify location, time and intensity measurements at landfall, and incorporating previously undocumented TCs (Landsea et al 2004). An easy-to-read HURDAT Best Track data file was created by Landsea in 2003 for ease of use in interpreting variables.

In 2004 the Extended Best Track (EBT) dataset was created to include size and structural parameters such as wind radii at the 34kt, 60kt and 74kt levels among each quadrant of the storm, radius of maximum wind (RMW) and Eye Diameter (ED) readings, as well as the pressure of the outmost closed isobar (POCI) that could be analyzed statistically throughout the storm quadrants (Kimball and Mulekar 2004; Demuth et al 2006). This information has been estimated for land-falling TCs from 1988-present for the North Atlantic Basin, with various size parameters available for select storms dating back to 1851.

For the purpose of this thesis, the easy-to-read HURDAT database available online (http://www.aoml.noaa.gov/hrd/hurdat/easyread-2012.html) was used to collect information for all land-falling TCs within the study area at the closest advisory time to landfall. Information extracted from this database included the date, time (in GMT), coordinate location and intensity (measured by the 1-minute maximum sustained wind speed) of the TC. In order to determine a possible relationship between size, intensity, and tornado output for a

land-falling TC, the speed and direction were also documented. The EBT dataset was also used to extract size parameters such as RMW, ED, and Radius of Outermost Closed Isobar, or ROCI, as they provide the best estimates when assessing storm size at given time periods (Kimball and Mulekar 2004).

d. Surface and Upper-Level Reanalysis Data Composites

In order to assess the environment conducive to multiple tornadoes among land-falling TCs, surface and upper-air composites were analyzed to determine similarities among select storms with high TCT and TLT output. Information was gathered from NOAA's Earth Science Research Laboratory's (ESRL) 6-Hourly Reanalysis composites dataset (http://www.esrl.noaa.gov/psd/data/composites/hour/). The synoptic composites analyzed included 850mb, 700mb, 500mb, and 200mb for the prolific tornado-producing storms with either high TCT or TLT output. In addition, select surface charts were extracted from substantial tornado-producing TCs to assess the environment at the time closest to TC landfall.

The surface chart is one of the most widely used tools among forecasters in meteorology and assesses numerous parameters, including temperature, dewpoint, current sky coverage, and winds at various observation locations in 6 hour intervals. Isobaric and frontal analyses are also performed at this level, including identifying trough axes and drylines (Vasquez 2003). The surface chart is important in observing changes among a TC during its lifecycle, including fluctuations in pressure and wind. As a TC nears landfall, an increase in tornado potential is possible, especially within the vicinity of a frontal boundary. Surface charts from Hurricanes Beulah (1967) and Ivan (2004) were extracted from NOAA's Central Library

which houses the U.S. Weather Maps Project – a collection of surface maps ranging from 1871-present which is available online (http://docs.lib.noaa.gov/rescue/dwm/data_rescue_daily_weather_maps.html; http://www.hpc.ncep.noaa.gov/dailywxmap/index.html). These TCs were chosen for analysis due to their extreme tornadic output coupled with their disparate tracks once inland. The results of these two TCs are discussed in Chapter 4.

The 850mb chart's primary usage, most notably during the spring months, is to locate the position of the low-level jet (LLJ), a "current" of fast-moving air which fluctuates from the southern coastline of the United States to the central portion of the country (Vasquez 2003). Severe weather, and thus, tornadic potential, is heightened if the LLJ is aligned to the right of a trough base, in which an increasing level of divergence is located. If aligned, the level of wind shear is intensified, which increases the probability of tornado formation.

Relative humidity (RH), a ratio expressing the amount of water vapor in the air relative to the water vapor capacity at a given temperature (Rauber et al 2008), can be examined using a variety of charts. The 700mb chart was used for analysis in this thesis (Vasquez 2003). High percentages of RH in the atmosphere are conducive to moisture and increased cloud cover. For land-falling TCs, this layer of the atmosphere is also used to determine areas of dry air intrusion, a factor imperative to the formation of tornadoes (Malkin and Galway 1953; Hill, Malkin and Schulz 1966; Schultz and Cecil 2009).

Large-scale systems, such as troughs and ridges, can be found by analyzing the 500mb chart (Vasquez 2003). It has been shown that tornado-producing TCs show an enclosed circulation with lower height values at this level (Cohen 2010). Areas of increased

divergence are located to the east of a trough axis, enhancing tornado production, while ridge patterns (associated with sinking air) hinder tornado formation, most notably to the east of a ridge axis.

An additional upper-level chart beneficial to the detection of tornadoes within land-falling TCs is the 200mb. At this level, the swift moving currents of the jet stream that promote uplift can be detected. The identification of jet maxes within the jet stream is where vertical lift is imminent, which is necessary in the formation of tornadoes.

In order to accomplish the second objective of this thesis, TCs with the highest TCT or TLT ratio (in other words, TCT output divided by TLT output for each TC) were chosen and synoptic charts were extracted using ESRL's dataset. Composites were created at the aforementioned height values near the time of tornado formation of each TC to examine the overall environment surrounding a tornado-producing TC and to determine the causes of high TCT or TLT output, respectively.

e. Upper-Level Sounding Data

In order to examine the tornadic environment accompanying a land-falling TC, a dynamic approach is necessary. Sounding data near time of formation was extracted using Plymouth State Weather Center's RAOB Selector for Archived Contiguous United States Data, available online (http://vortex.plymouth.edu/raob_conus-u.html). Because RAOB data is obtained twice daily (00Z and 12Z) and in limited locations, the dynamic information was gathered at the location, time, and date closest to tornado occurrence. Specific parameters assessed included CAPE, total SRH, EHI, BRN, K-Index, and SWEAT Index. Each parameter assesses some aspect of thunderstorm and tornado formation potential within the

atmosphere and is an important factor when identifying tornado outbreaks. An index of values among each parameter is listed in Appendix A.

Convective Available Potential Energy, or CAPE, includes the area on a thermodynamic sounding in which the parcel temperature is warmer than the environment within all height levels of the troposphere (Rauber et al 2008). CAPE is examined to determine the amount of instability within the atmosphere at a given location. The greater the instability, the better chance of air parcels rising freely without force, which is beneficial for a potentially tornadic environment (NWS 2004).

Total Storm Relative Helicity, denoted as either SRH or Hs-r, is the amount of vertical and directional wind shear within the lower atmosphere relative to thunderstorm movement. High amounts of SRH are conducive to strong rotation and supercell formation (Rauber et al 2008). Furthermore, SRH is a major component of Energy Helicity Index (EHI). The EHI is a product of CAPE and SRH, divided by 160,000, in which higher values denote the potential for strong updrafts, increasing tornadogenesis within the development of supercells and mesocyclones (NWS 2004).

Bulk Richardson Number (BRN) examines the balance between CAPE and shear within a thunderstorm environment. Thermodynamic soundings that involve high CAPE readings will see a high BRN. Low values of BRN indicate a shear-driven environment. Supercells are likely with low BRN values, with a greater probability within the 10-45 range, increasing the potential for tornadoes (NWS 2004).

The K-Index and Severe WEAther Threat (or SWEAT) Index examine the convective and severe weather potentials, respectively. The K-Index assesses the differences between

three parameters among three height values – the 850mb (temperature and dewpoint), 700mb (dewpoint depression) and 500mb (temperature) charts. Higher values denote higher convective potential. The SWEAT Index measures the severe weather threat utilizing a variety of variables, including temperature at various heights, dewpoint, and shear. As with most indices, a higher value denotes a greater chance of severe weather and associated tornadoes, most notably if SWEAT values are over 400.

3.3 Statistical Analysis

SPSS software Version 19 was used to explore relationships between TC size, intensity, and tornado output. Simple descriptive statistics were used to examine the dynamic parameters observed when determining potential tornado outbreaks.

3.3.1 TC Size, Intensity and Tornado Output

a. Multiple Linear Regression

It is important to note that multiple linear regression was attempted to assess relationships between the variables. Only 88 TCs contained the information that was needed, therefore this test was attempted to predict the missing ROCI values based on other variables. This was unsuccessful so missing values were deleted. Furthermore, multiple linear regression was used to determine specific relationships between the various size parameters gathered (ROCI, ED, and RMW) at landfall as well as intensity and total tornado output within the study area. As a result of missing information, only 14 storms within the dataset contained the data necessary to perform the test. Due to small sample size, results were unsuccessful.

b. 2-way ANOVA

A 2-way ANOVA was performed to evaluate the effects of TC size and intensity on tornado output within the study area. This test was used to determine two things: 1) if each independent variable or factor had an individual effect (or main effect) on the dependent variable and 2) if each independent variable had any effect upon the other (defined as interaction effect).

Two-way ANOVA requires the same sample size within each variable to be tested. Therefore, a total of 89 TCs within the dataset were used for analysis, as data was available for each TC. Each independent variable was categorized into groups. ROCI size at landfall was divided into two groups based on the overall median ROCI measurement: small (0-175 nm) and large (>175 nm). A total of 47 TCs were categorized as small while 42 TCs fell into the large group. Intensity values were divided into three categories roughly based on SS hurricane wind categories: 'weak' (39-74 mph), 'minor' (75-115 mph) and 'major' (>115 mph). Overall, 41 TCs were listed as 'weak', 25 'minor', and 23'major'. Tornado output includes only those that made landfall within the study area; therefore, it may not represent the total count of all tornadoes in association with a land-falling TC.

The 2-way ANOVA test was performed a second time, with the tornado count for the 15 most prolific tornado-producing TCs adjusted to include all tornadoes spawned within their corresponding life cycles. This was performed for comparison purposes only; to see if any changes occurred in the relationships between the variables. Any significant changes to the output within this study would be primarily affected by the top 15 tornado-producing TCs.

c. General Linear Model

A general linear model was generated to assess tornado output among the two independent variables, TC size (ROCI value at landfall) and intensity (at landfall). For this test, the independent variables were used as covariates with all variables displayed as a continuous distribution. This test was used to determine the possibility of a linear relationship between the estimated tornado output average among intensity and size variables as well as the variability of tornado output among each independent variable.

3.3.2 Dynamic Analysis of Tornado Output

General inferential statistics were used to describe the dynamic environment among select TCs with high TCT or TLT output (Table 4). In order to capture the environment that best represents a TC's respective tornado production, TCs with the highest TCT to TLT ratio (in other words, TCT output divided by TLT output for each TC) were chosen. To assess normality among the given sample size, a Kolmogorov-Smirnov test was performed. An independent samples t-test as well as a Mann-Whitney U test was executed to determine the significance of select parameters between TCT and TLT storms. For example, dynamic parameters such as K-Index, SWEAT Index, CAPE, SRH, BRN and EHI were chosen for analysis within the study. For the purpose of this objective, the dynamic parameters among the select storms were tested to determine differences between each group, which provided a basis as to the values most applicable to tornado production within the two groups.

Table 4: TCs with higher TCT or TLT output.

Tropical Cyclone	TCT Output	TLT Output
Hurricane Beulah (1967)	117	0
Hurricane Rita (2005)	104	0
Hurricane Ivan (2004)	49	5
Hurricane Georges (1998)	35	14
Hurricane Katrina (2005)	49	0
Hurricane Andrew (1992)	42	6
Hurricane Gilbert (1988)	39	0
Hurricane Allen (1980)	34	0
Hurricane Ike (2008)	33	0
Hurricane Danny (1985)	20	11
Hurricane Cindy (2005)	17	11
Hurricane Lili (2002)	26	1
Hurricane Audrey (1957)	22	1
Hurricane Alicia (1983)	22	0
Hurricane Carla (1961)	20	1
Tropical Storm Fay (2008)	14	20
Tropical Storm Bill (2003)	6	9
Tropical Storm Fay (2002)	3	8
Tropical Storm Hermine (2010)	3	8
Tropical Storm Chris (1982)	3	6
Tropical Storm Frances (1998)	3	6
Tropical Storm Candy (1968)	2	5
Tropical Storm Allison (1989)	1	8
Tropical Storm Debra (1978)	1	3
Tropical Storm #1 (1960)	1	2
Hurricane Bonnie (1986)	0	5
Tropical Storm #1 (1964)	0	3
Tropical Storm Jenny (1969)	0	2
Tropical Storm Becky (1970)	0	2
Tropical Storm Beryl (1994)	0	2

4. Results

4.1 TC Size, Intensity and Tornado Output

a. 2-way ANOVA

Out of the 95 total TCs within this study, 89 were used to determine relationships between TC size, intensity, and tornado output (Table 5). With the TC dataset divided into intensity and size, the majority of tornadoes associated with TCs spawned from storms listed as ‘weak’ in intensity (46%), followed by ‘minor’ (28%) and ‘major’ (26%) (Figures 3 and 4). Upon assessing size, the majority of tornadoes spawned within TCs that were categorized as small. This confirms research from previous climatologies (McCaul 1991; Edwards 2010).

Table 5: All tropical cyclones with given intensity, size and tornado output in the study area.

Tropical Cyclone	Intensity	Size	Output	Tropical Cyclone	Intensity	Size	Output
Hurricane Camille (1969)	major	large	2	Hurricane Edith (1971)	minor	small	16
Hurricane Eloise (1975)	major	large	5	Hurricane Cindy (2005)	minor	small	28
Hurricane Betsy (1965)	major	large	6	Hurricane Danny (1985)	minor	small	31
Hurricane Carmen (1974)	major	large	6	Tropical Storm Hazel (1953)	weak	large	1
Hurricane Hilda (1964)	major	large	7	Hurricane Ethel (1960)	weak	large	1
Hurricane Wilma (2005)	major	large	8	Tropical Storm Keith (1988)	weak	large	2
Hurricane Dennis (2005)	major	large	9	Tropical Storm Harvey (1999)	weak	large	2
Hurricane Elena (1985)	major	large	9	Tropical Storm Becky (1970)	weak	large	2
Hurricane Frederic (1979)	major	large	10	Tropical Storm Hermine (1998)	weak	large	2
Hurricane Opal (1995)	major	large	19	Tropical Storm Marco (1990)	weak	large	2
Hurricane Carla (1961)	major	large	21	Hurricane Abby (1968)	weak	large	4
Hurricane Audrey (1957)	major	large	23	Hurricane Gordon (1994)	weak	large	5
Hurricane Gilbert (1988)	major	large	39	Hurricane Mitch (1998)	weak	large	6
Hurricane Katrina (2005)	major	large	49	Tropical Storm Frances (1998)	weak	large	9
Hurricane Ivan (2004)	major	large	54	Hurricane Isidore (2002)	weak	large	10
Hurricane Rita (2005)	major	large	104	Hurricane Gabrielle (2001)	weak	large	19
Hurricane Beulah (1967)	major	large	117	Tropical Storm Fay (2008)*	weak	large	34
Hurricane Bret (1999)	major	small	6	Tropical Storm Hannah (2002)	weak	small	1
Hurricane Celia (1970)	major	small	8	Tropical Storm Arlene (1959)	weak	small	1
Hurricane Charley (2004)	major	small	17	Tropical Storm Matthew (2004)	weak	small	1
Hurricane Alicia (1983)	major	small	22	Tropical Storm Beryl (1994)	weak	small	2
Hurricane Allen (1980)	major	small	34	Tropical Storm Claudette (1979)	weak	small	2
Hurricane Andrew (1992)	major	small	48	Tropical Storm #1 (1965)	weak	small	2
Hurricane Claudette (2003)	minor	large	2	Hurricane Judith (1959)	weak	small	2
Hurricane Flossy (1956)	minor	large	3	Tropical Storm Dean (1995)	weak	small	2
Hurricane Irene (1999)	minor	large	4	Hurricane Bob (1985)	weak	small	2
Hurricane Dolly (2008)	minor	large	5	Tropical Storm Erin (2007)	weak	small	2
Hurricane Earl (1998)	minor	large	9	Tropical Storm Jenny (1969)	weak	small	2
Hurricane Juan (1985)*	minor	large	13	Tropical Storm Alberto (2006)	weak	small	3
Hurricane Agnes (1972)	minor	large	17	Tropical Storm Debra (1978)	weak	small	4
Hurricane Gustav (2008)	minor	large	19	Hurricane Fern (1971)	weak	small	5
Hurricane Lili (2002)	minor	large	27	Tropical Storm Delia (1973)*	weak	small	5
Hurricane Ike (2008)	minor	large	33	Tropical Storm Danielle (1980)	weak	small	5
Hurricane Georges (1998)	minor	large	49	Tropical Storm Bonnie (2004)	weak	small	6
Hurricane Humberto (2007)	minor	small	1	Hurricane Allison (1995)	weak	small	7
Hurricane Debra (1959)	minor	small	2	Hurricane Gordon (2000)	weak	small	7
Hurricane Gladys (1968)	minor	small	2	Tropical Storm Candy (1968)	weak	small	7
Hurricane Bob (1979)	minor	small	2	Tropical Storm Chris (1982)	weak	small	9
Hurricane Danny (1997)	minor	small	2	Tropical Storm Allison (1989)	weak	small	9
Hurricane Florence (1988)	minor	small	4	Tropical Storm Helene (2000)	weak	small	10
Hurricane Chantal (1989)	minor	small	4	Tropical Storm Hermine (2010)	weak	small	11
Hurricane Bonnie (1986)	minor	small	5	Tropical Storm Fay (2002)	weak	small	11
Hurricane Erin (1995)	minor	small	5	Tropical Storm Bill (2003)	weak	small	15
Hurricane Jerry (1989)	minor	small	7	Tropical Storm Allison (2001)*	weak	small	15
Hurricane Babe (1977)	minor	small	13	* denotes initial landfall			

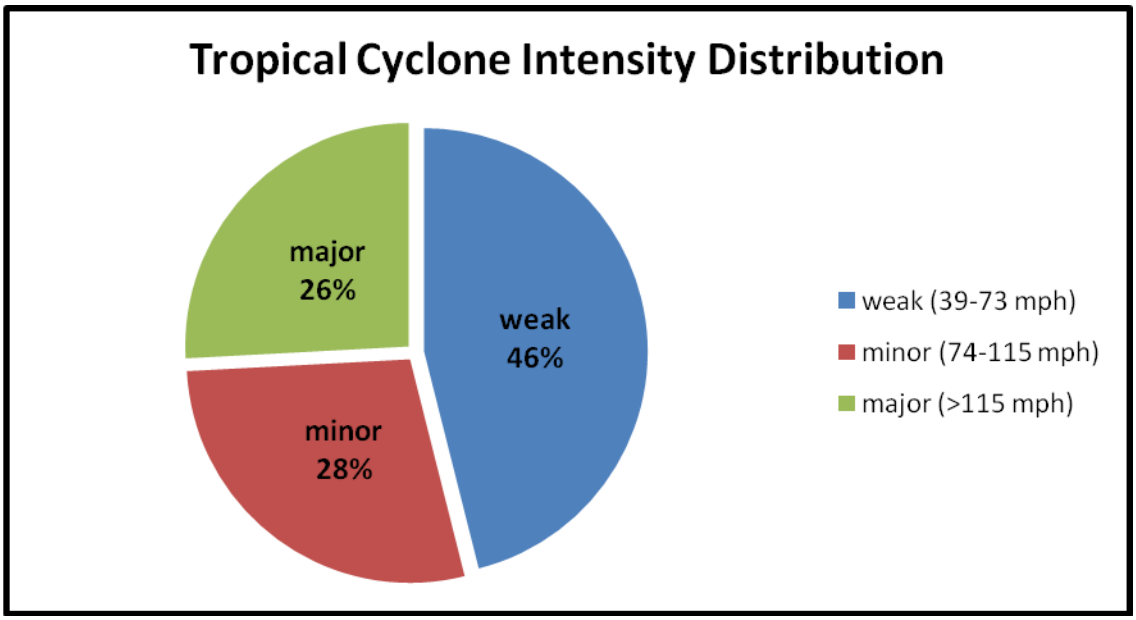

Figure 3: Tropical cyclone intensity distribution in study area.

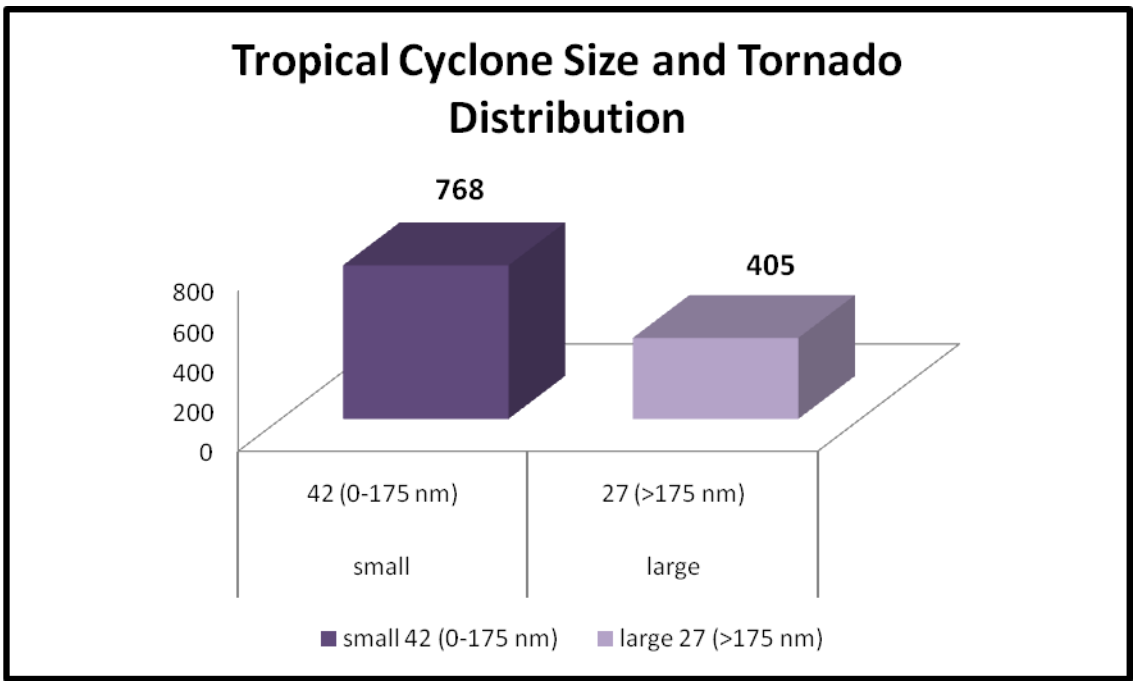

Figure 4: Tornado distribution and tropical cyclone size.

When testing for main effects, it was determined that intensity had a statistically significant effect on tornado output within the study area, with a p-value of < .01 (alpha level

of .05). When examining multiple comparisons among the various levels of intensity (Table 6), the mean differences between 'major' and 'minor' TCs, along with 'major' and 'weak' TCs were significant, with p-values of .011 and <.01, respectively. In other words, TCs categorized as 'major' produced a significantly greater amount of tornadoes than 'minor' and 'weak' when analyzed separately. No significant relationship, however, existed between 'minor' and 'weak' categorized TCs. A small non-significant influence can be seen between size and tornado output, given a p-value of .211. This influence shows that tornado output has the potential to be abundant in TCs that are categorized as large in size, but is not necessarily the case among all large TCs. In other words, large TCs can produce very few tornadoes, as with the case of Hurricane Claudette (2003), or an abundant amount, as seen in Hurricane Beulah (1967). No relationship could be determined analyzing the interaction effects of intensity and size on tornado output within the study area.

Table 6: Results of 2-way ANOVA, Adjusted 2-way ANOVA, and General Linear Model. Those marked with an asterisk (*) denote significance at the .05 level.

2 way ANOVA	
Intensity and tornado output	<.01*
Mean difference between 'major' and 'minor' TC intensity	0.011*
Mean difference between 'major' and 'weak' TC intensity	<.01*
Size and tornado output	0.211

Adjusted 2 way ANOVA	
Intensity and tornado output	<.01*
Mean difference between 'major' and 'minor' TC intensity	0.014*

General Linear Model	
Intensity and tornado output	<.01*
Size and tornado output	0.206

* significant at the .05 level

The results of these relationships are shown in Figure 5. Regardless of size, TCs categorized as ‘weak’ produced a low average tornado total, with increasing output as intensity increased. This relationship is not absolute, however, as many TCs of higher intensity values within the study area (eg. Category 4 and 5) produced relatively few tornadoes (e.g. Hurricanes Betsy (1965) and Camille (1969)). A large majority of TCs with Category 3 intensity spawned a substantial amount of tornadoes (Figure 6). This category was placed under ‘major’ for intensity, which may explain the results of this relationship. The results echo that of Moore and Dixon (2011), who state that there is a statistically significant relationship between TC intensity and tornado output, however, the majority of tornadoes were associated with Category 3 storms.

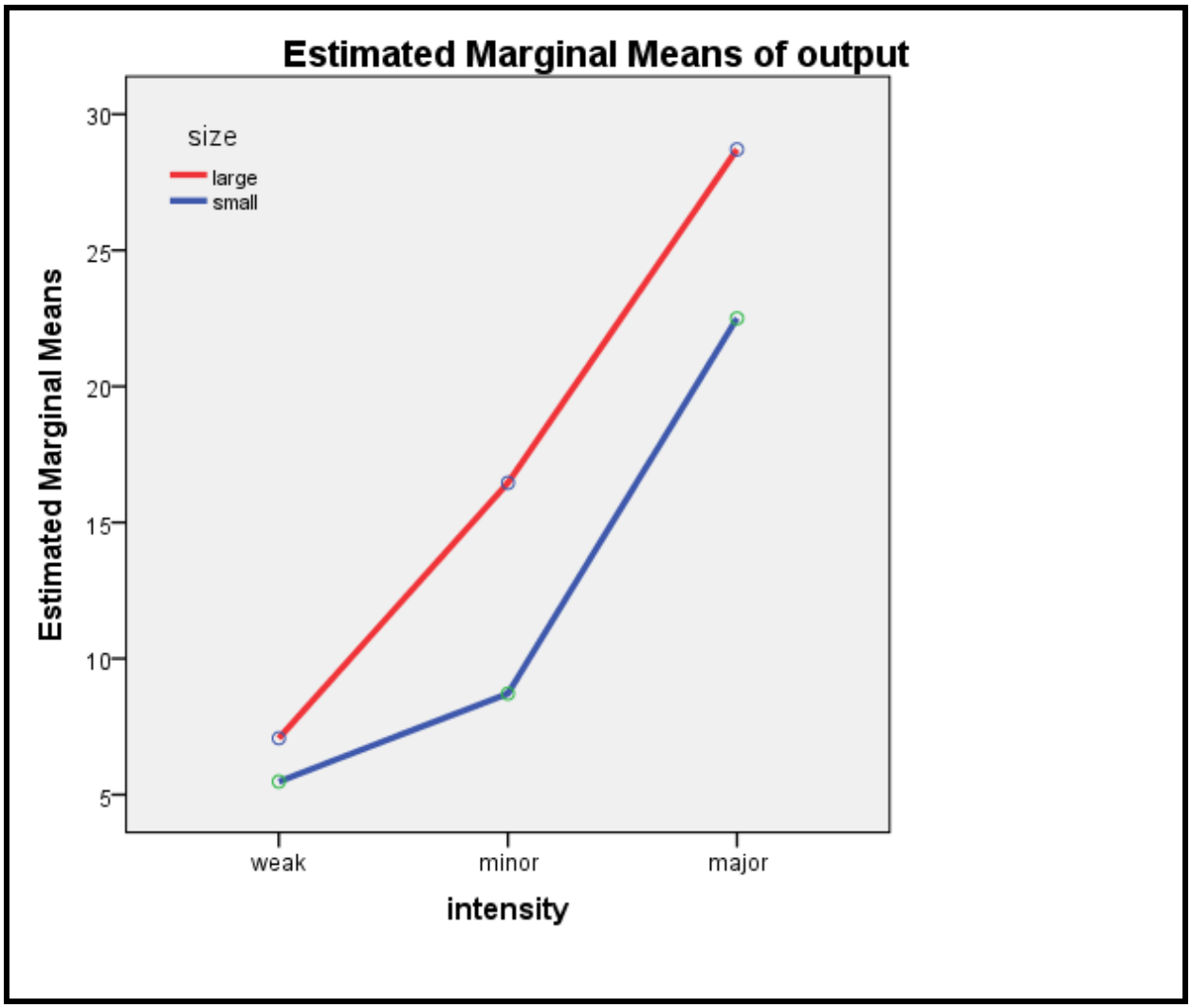

Figure 5: 2-way ANOVA profile plot depicting average tornado output and intensity with given size parameters. In general, average tornado output increases as intensity increases.

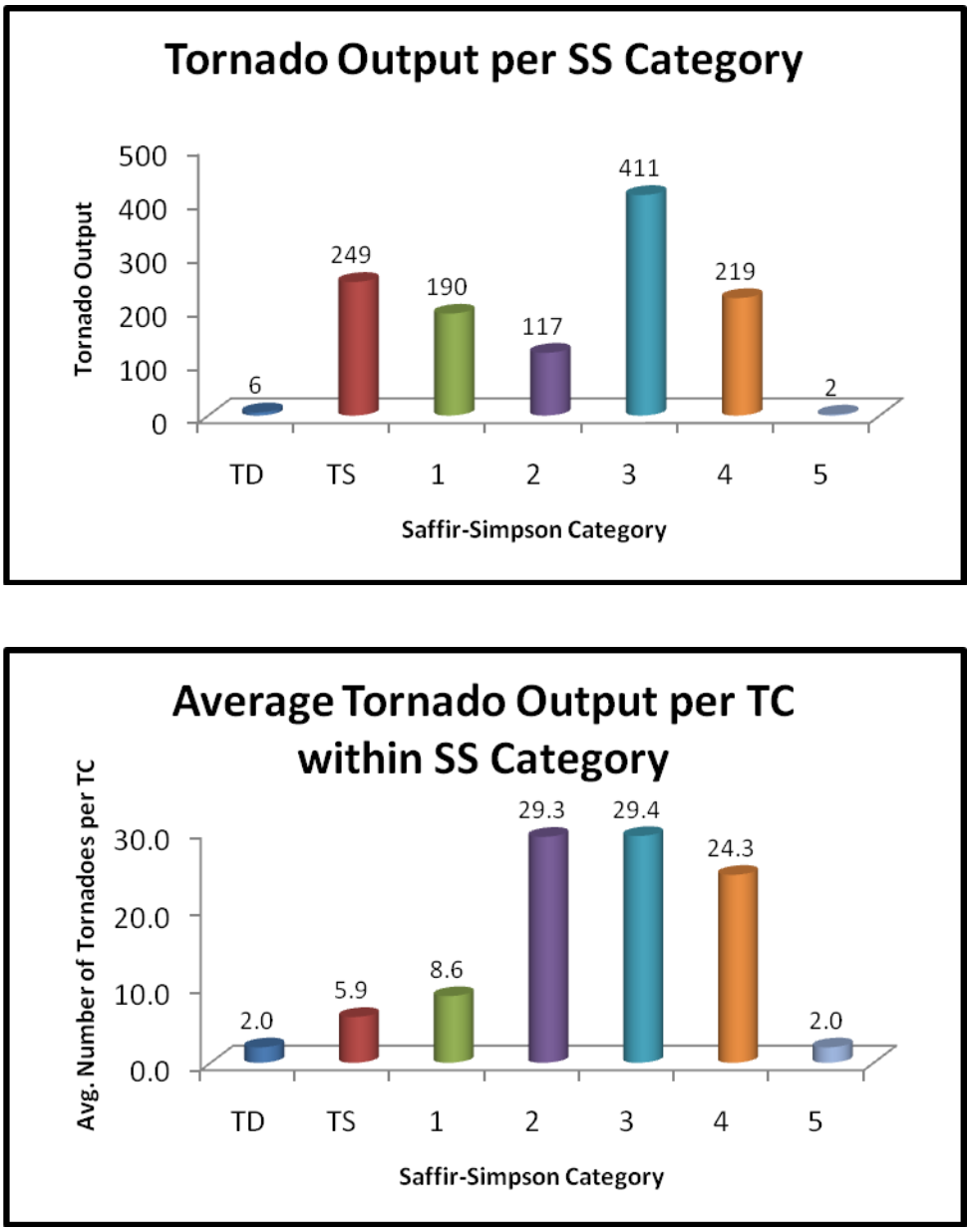

Figure 6: Top chart: Tornado output per SS category. Tornado output highest among Category 3 storms, with a total of 411 during the study period. Bottom chart: Tornado output per storm among SS category. Average number of tornadoes is higher among Category 2 and 3 TCs, with approximately 29 tornadoes within any given TC.

b. Adjusted 2-way ANOVA

The 2-way ANOVA was performed a second time, with tornado output adjusted for the 15 most tornado-prolific storms in the dataset (Table 7). The original dataset for this sample

included only tornadoes that spawned within the study area. This adjustment was made to include all tornadoes within the life cycle of the TC, as these 15 TCs would possibly show the greatest amount of variance within the dataset.

Table 76: Adjusted tornado output for 15 most prolific tornado-producing TCs.

Tropical Cyclone	Intensity	Size	Original Output	Adjusted Output
Hurricane Beulah (1967)	major	large	117	117
Hurricane Rita (2005)	major	large	104	104
Hurricane Ivan (2004)	major	large	54	118
Hurricane Katrina (2005)	major	large	49	59
Hurricane Georges (1998)	minor	large	49	49
Hurricane Andrew (1992)	major	small	48	49
Hurricane Gilbert (1988)	major	large	39	41
Tropical Storm Fay (2008)	weak	large	34	50
Hurricane Allen (1980)	major	small	34	34
Hurricane Ike (2008)	minor	large	33	33
Hurricane Danny (1985)	minor	small	31	33
Hurricane Cindy (2005)	minor	small	28	48
Hurricane Lili (2002)	minor	large	27	27
Hurricane Audrey (1957)	major	large	23	23
Hurricane Alicia (1983)	major	small	22	22

Results show a minute decrease in significance between the variables; however, intensity and tornado output remain significant, with a p-value of $< .01$ (Table 6). When assessing multiple comparisons, the only change resulted within mean intensity differences between ‘major’ and ‘minor’ TCs, with a p-value of .014. When examining the adjusted 2-way ANOVA graph (Figure 7), results display minor modifications, with a slight decrease in tornado output of ‘minor’ intensity TCs, increasing the ‘weak’ and ‘major’ intensity averages among large TCs. Therefore, the assumptions remain that large storms of ‘major’ intensity are more likely to produce tornadoes than small storms categorized as ‘minor’ or ‘weak’.

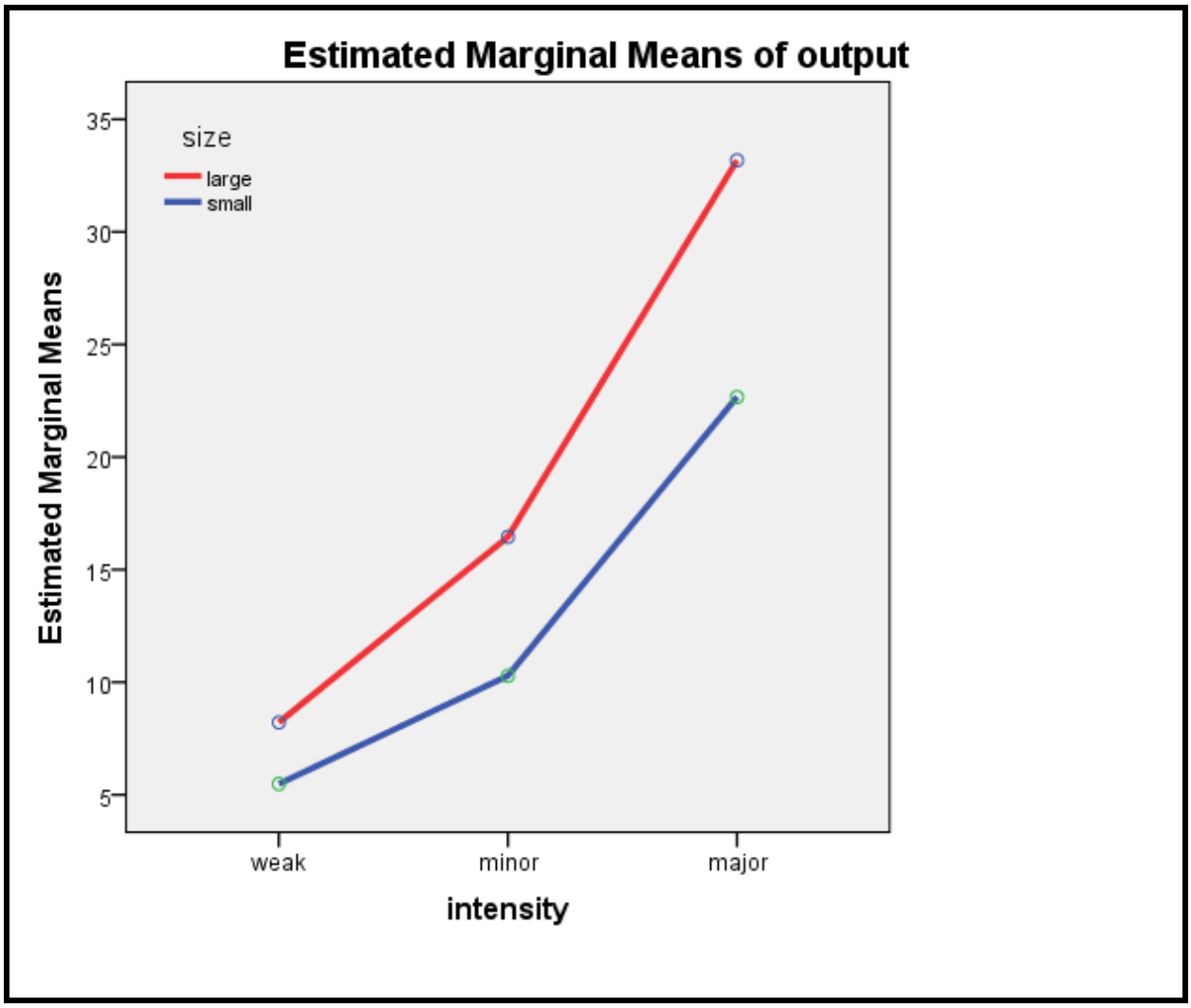

Figure 7: Adjusted 2-way ANOVA profile plot. Results display average tornado output to be greater among TCs listed as 'major' in intensity. After adjustment, average tornado output slightly strengthened among the 'weak' and 'major' categories.

c. General Linear Model

A general linear model was also attempted to determine whether tornado output could be predicted based on size and intensity variables. Main effects display similar results to 2-way

ANOVA, in which significance can be found among intensity and tornado output (p-value < .01). Tornado output remained only slightly influenced by size (p-value = .206) (Table 6). This result is further displayed when examining the estimated mean scatterplots shown in Figure 8. From the scatterplot matrix, it can be seen that only TC intensity and output display a correlation, revealing that high-intensity TCs generally spawn a greater amount of tornadoes. On the other hand, TC intensity and size as well as size and tornado output show no relationships amongst each other.

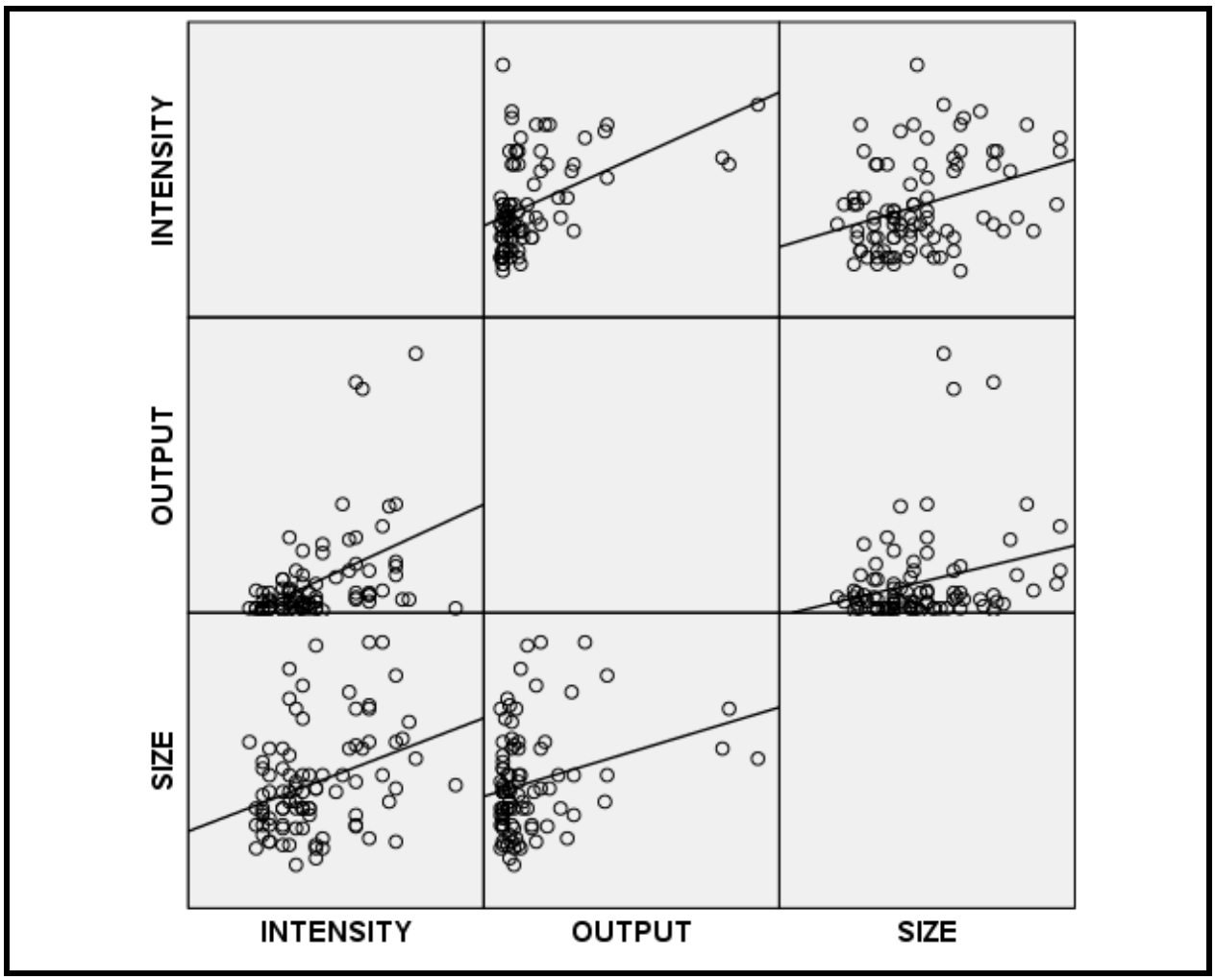

Figure 8: Profile line plot for estimated means. Results from this scatterplot matrix show only a relationship between intensity and tornado output; TCs of high intensity produce (on average) a high tornado output.

The residual plot in Figure 9 displaying observed and predicted values shows no clear relationships when analyzing tornado output against both independent variables. It can be seen in the plot located within the center column of the final row that variability among size and intensity increases as tornado output increases, displaying signs of heteroscedasticity. Thus, TC size and intensity are not good predictors of TC tornado output using linear modeling methods.

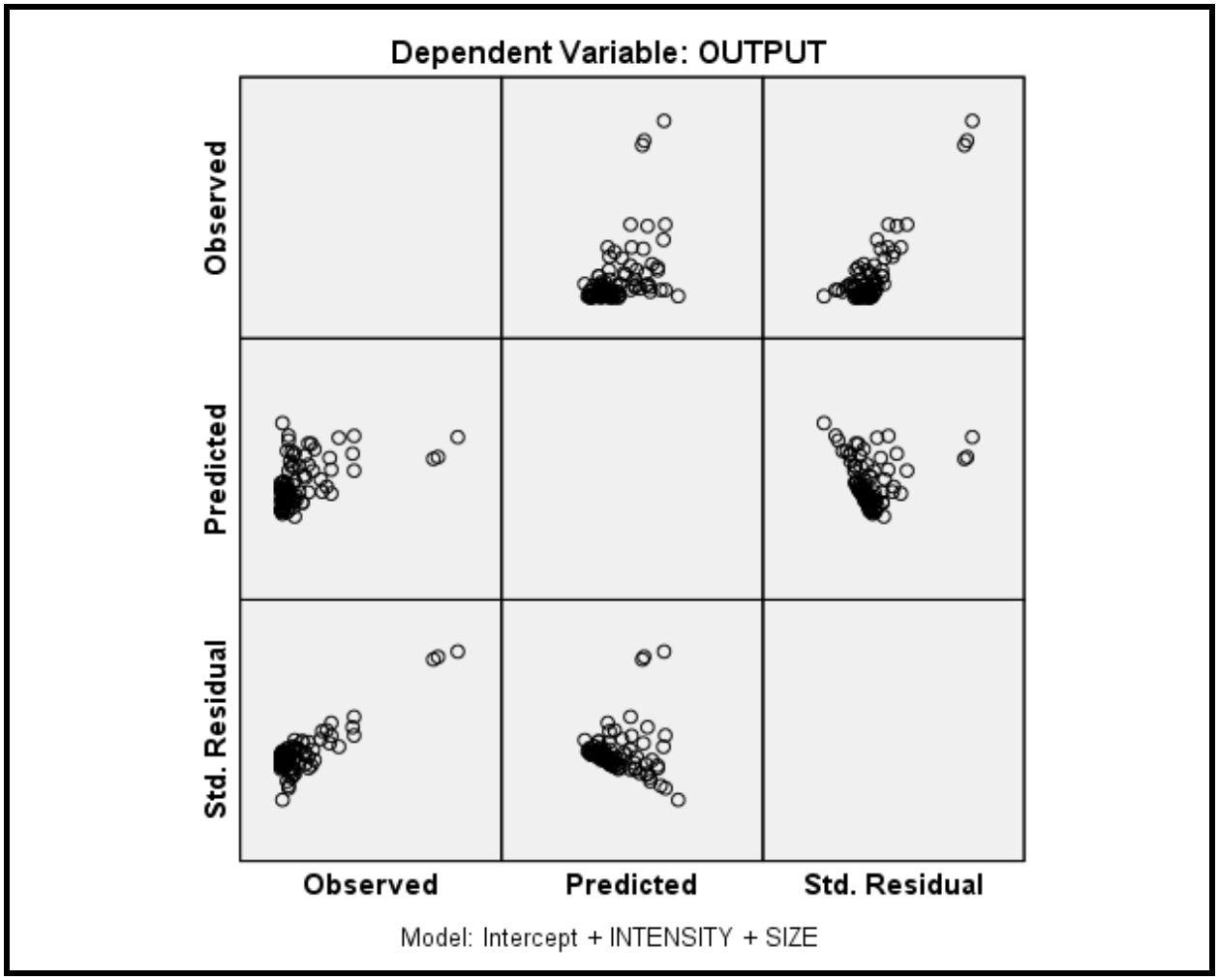

Figure 9: Residual plot displaying relationship between tornado output among both intensity and size. Outcomes display an increase in variability among the independent variables as tornado output decreases.

4.2 Synoptic and Dynamic Analysis of Tornado Output

a. Surface and Upper-Level Reanalysis Data Composites

Synoptic composites were created at the time and date closest to tornado formation using 15 TCs with higher TCT output along with 15 TCs containing greater TLT. Out of the 17 TCs that produced more tornadoes as a tropical depression or remnant low (TLT phase), those that produced greater than 1 tornado were chosen. Single tornado-producing TCs can be attributed more to chance, therefore acquiring a sample that is best representative of the population of tornadoes produced within this phase.

Beginning with the 850mb composite among TCT (Figure 10), it can be seen that low-level wind shear is heightened among greater tornado-producing TCs, with higher average shear values peaking at 9 m s^{-1}. Furthermore, the increased values are located northeast of the center of circulation for the prolific tornado-producing events (TC location not displayed). Vector winds show an onshore flow pattern, streaming from the Gulf of Mexico. The small increases in low-level shear values, most notably in the south-central portion of Texas, are primarily due to the right-front quadrant locations of Hurricanes Gilbert (1988) and Allen (1980), which are areas favorable for tornado development. This is not the case, however, among TLT composites, in which average shear values are lower (6 m s^{-1}) and oriented in a more N-S direction below the center of circulation for the weaker tornado-producing TCs (Figure 11).

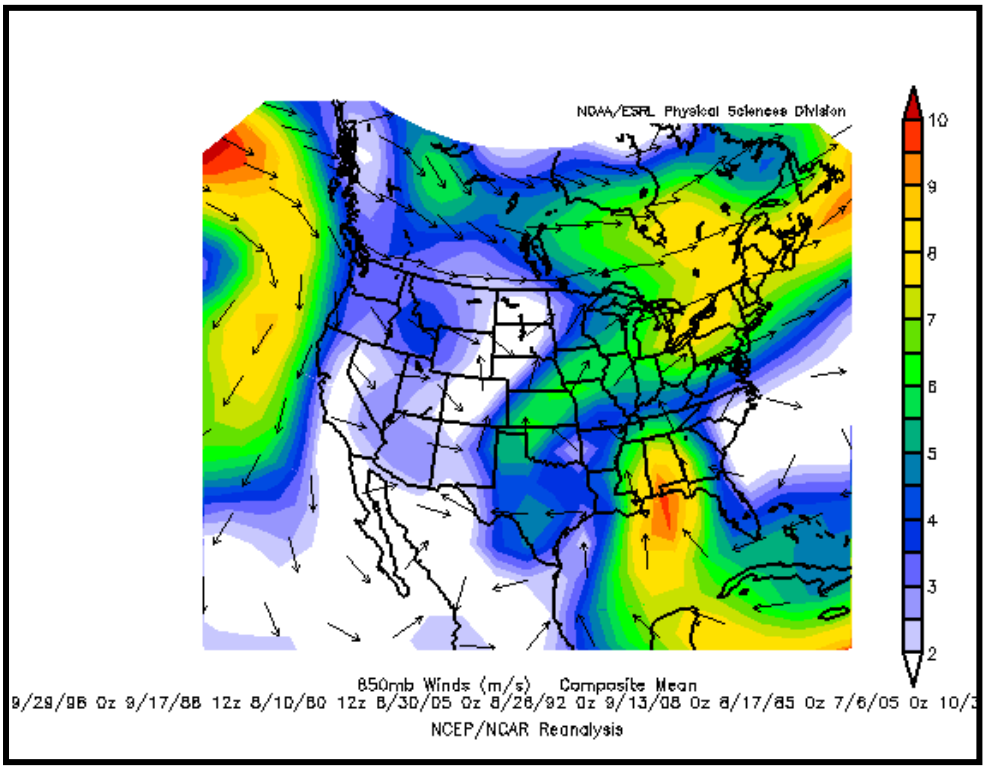

Figure 10: 850mb mean composite for TCT. Higher wind shear values are shown in areas of prolific tornado occurrence.

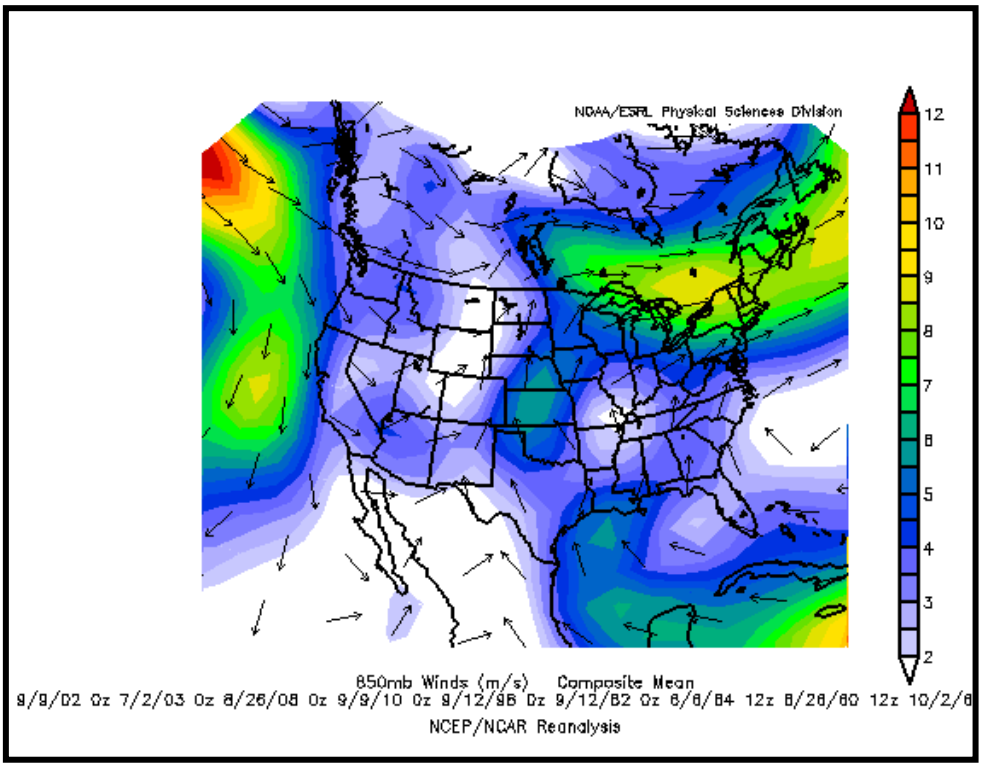

Figure 11: 850mb mean composite for TLT. Average wind shear values are lower within weaker tornado-producing TCs.

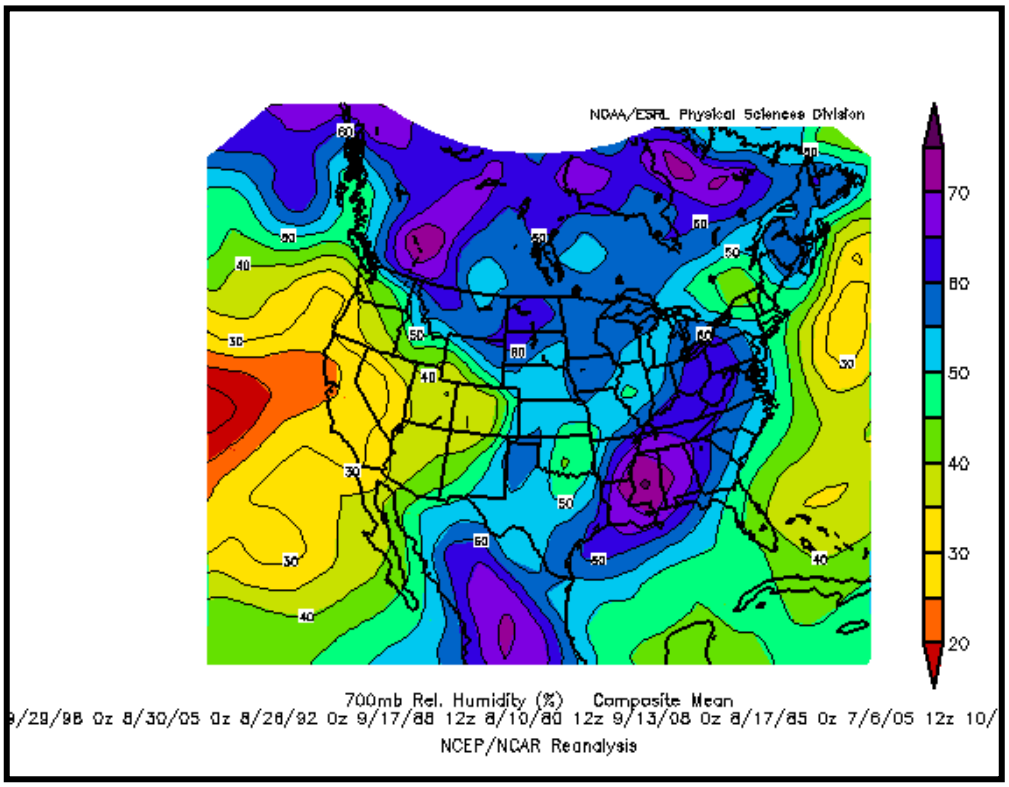

Figure 12: 700mb mean composite for TCT environment. Higher amounts of RH can be detected within the area of TC. Evidence of dry air intrusion is also visible.

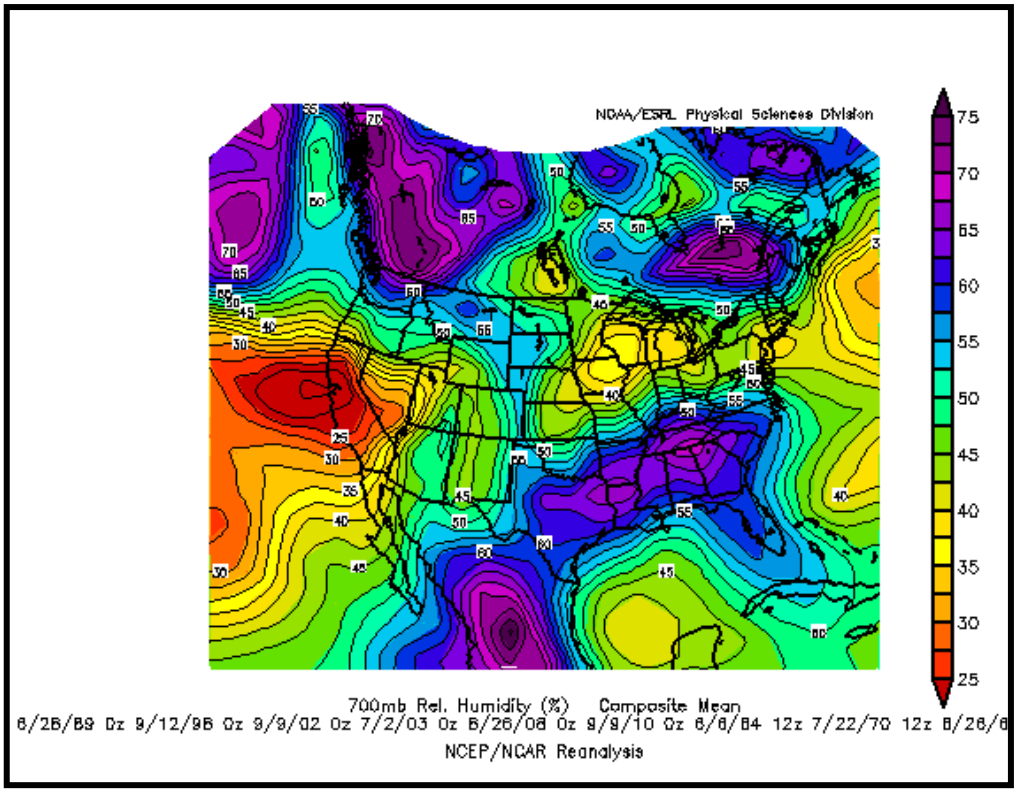

Figure 13: 700mb mean composite for TLT environment. Broad area of high RH percentages inhibit dry air intrusion and subsequent tornado formation.

Upon assessment of the 700mb chart for TCT (Figure 12), it can be seen that an elongated area of RH is located in the same general vicinity as 850km wind shear, with a SW-NE orientation. A tighter gradient in RH values can be seen in the northwestern quadrant in relation to the highest RH values, indicative of the presence of dry air intrusion into the TC. This dry air intrusion weakens the TC itself, yet enhances the formation potential of tornadoes within its structure by increasing the buoyancy which in turn decreases cloud cover, allowing a greater amount of insolation into the region.

The 700mb chart for TLT, however, exhibits a widely displaced amount of RH, with increased values along the Texas-Louisiana border and near the vertex of the Alabama, Tennessee and Georgia state lines (Figure 13). Like the TCT environment, the gradient in the northwest quadrants of highest RH display evidence of dry air intrusion, which may shed light on the development of tornadoes that were spawned within the select TCs. However, the broad area of high RH values over a large portion of the southeast potentially hindered buoyancy and subsequent tornadogenesis within the TC.

Ridge and trough patterns are clearly defined in the 500mb composites for both TCT and TLT outputs (Figures 14 and 15). Within the TCT environment, a ridge is visible along the eastern coastline of the United States, with increasing height values extending into the Atlantic Ocean. All TCs were located to the west of the ridge axis, which potentially aided in storm recurvature, further supporting prolific tornado output. Among the TLT environment (Figure 15), the trough axis situated close to the Texas-Louisiana border resulted in some tornado output near the area of strongest divergence. Within this pattern, Tropical Storms Frances (1998) and Fay (2002) spawned a combined 20 tornadoes along the Louisiana and Texas coasts (not pictured).

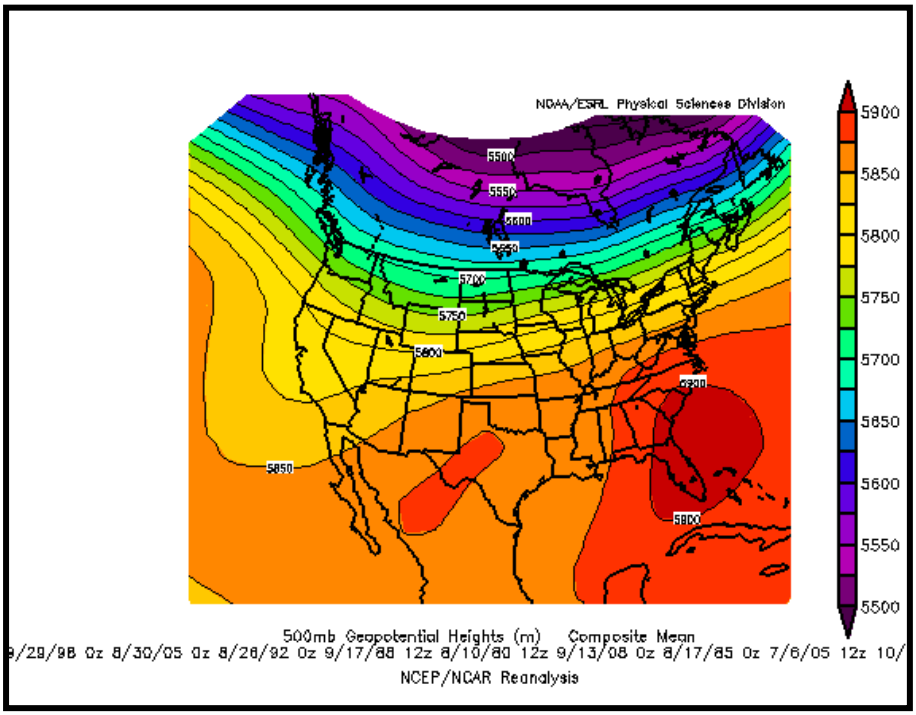

Figure 14: 500mb composite for TCT environment. A defined ridge in the western Atlantic may aid in storm recurvature, increasing tornado output within this phase.

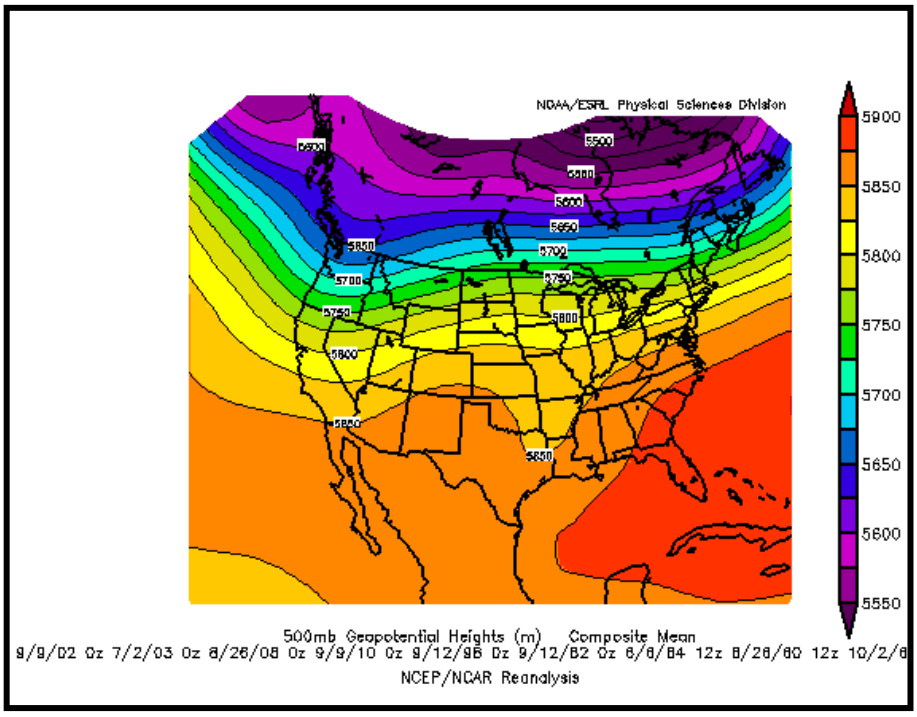

Figure 15: 500mb mean composite for TLT environment. Trough over the Louisiana-Texas border is the leading cause for tornado output among select storms in study period.

The 200mb charts for both TCT and TLT were analyzed to determine the location of the jet stream in relation to TC position at time of analysis. The jet stream consists of a river of fast-moving air that may also include embedded regions of faster winds called jet streaks. It can be seen within the TCT composite that the jet stream is situated farther south, above a broadened ridge centered northwest of the Ohio Valley (Figure 16). This location is northeast of the center of TC circulation for the majority of TCs analyzed within the TCT phase. Therefore, the positioning places the TCs within the vicinity of the right entrance region of the jet streak, commonly associated with rising air and increased divergence, which further aids in the development of tornadoes. The TLT phase composite, on the other hand (Figure 17) shows a jet stream that is situated further north than that of the TCT phase, with areas of faster winds separated within the flow. These regions are displaced from the majority of TC locations, hindering interaction and lessening tornado potential. In addition, the majority of TCs are positioned underneath a pronounced ridge within the Southern Plains, which is synonymous with sinking air, prohibiting the convection necessary for the formation of tornadoes.

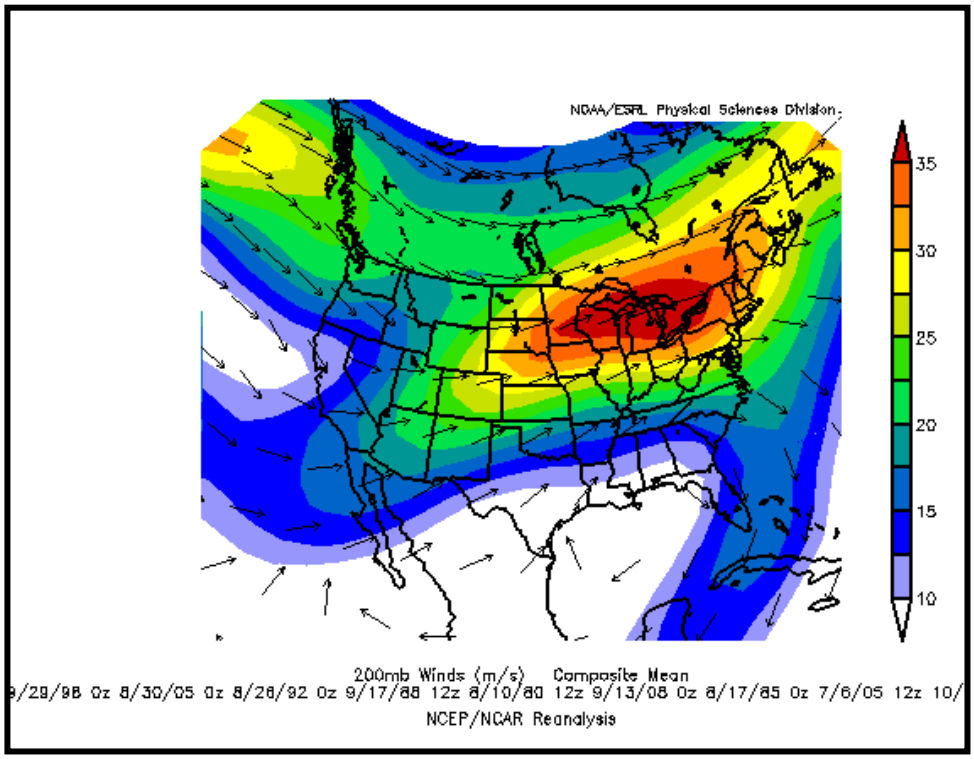

Figure 16: The 200mb mean composite shows the jet stream with an embedded jet streak positioned north of the Ohio Valley. The location of the right entrance region to the northwest aids in upper-air divergence, increasing the probability of tornadoes to occur within this phase.

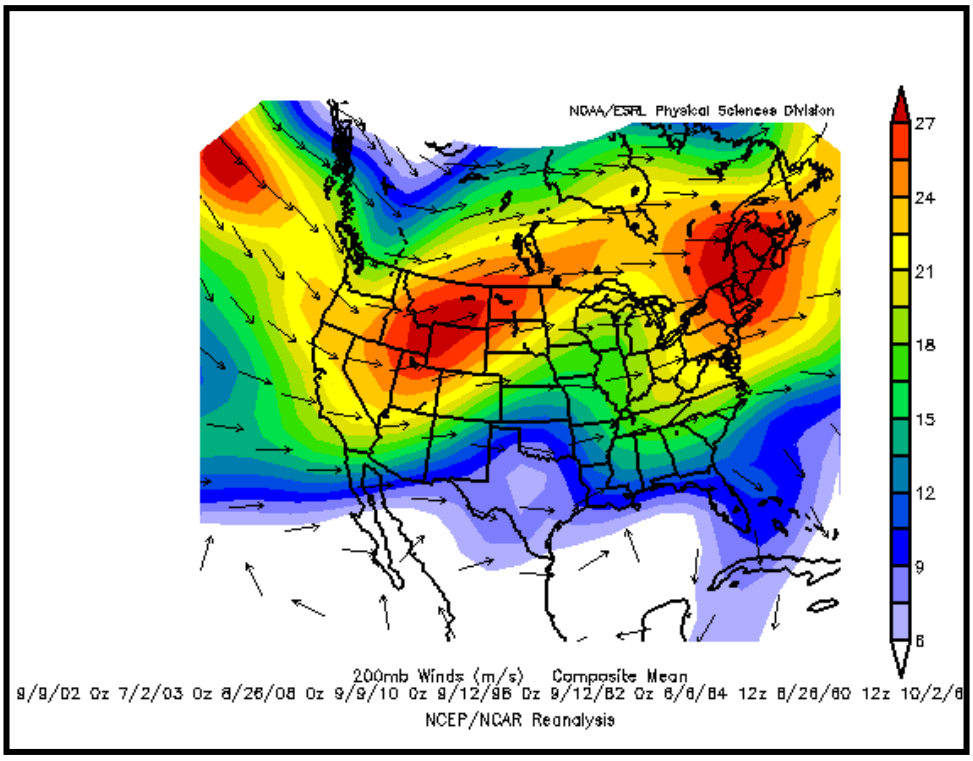

Figure 17: The 200mb mean composite for TLT shows the jet stream positioned much higher than that within the TCT environment, with max wind values displaced among the stream, decreasing the probability of tornadoes to occur.

To understand the reasoning surrounding the abundance of tornadoes that were produced within the lifecycles of Hurricanes Beulah (1967) and Ivan (2004), their respective surface charts were selected for analysis (Figures 18 and 19). As can be seen among Beulah (1967), a stationary front was positioned to the northwest of the center of circulation on the day of landfall. This front and the air mass behind it hindered advancement of Beulah's track further inland. The observation two days post-landfall shows the stationary front transitioned to a cold front pressing southwestward. Additionally, high-pressure systems were positioned to the north and northwest of Beulah's circulation. Beulah's sharp turn towards the southwest likely resulted from the frontal position and subsequent movement (towards the southwest) as well as the positioning of the various high-pressure systems around the circulation. Orton (1970) adds that the abundance of tornadoes was likely due to 1) time of day, with the majority of tornadoes spawning in the morning and early afternoon hours, 2) orientation of the storm to the Texas coastline, and 3) the length of time Beulah remained along the coast before movement inland.

Frontal boundary influence was also associated with Hurricane Ivan (2004). Upon landfall on September 16, 2004, a cold front was situated northwest of Ivan's circulation and pushing eastward (Figure 19). The observations that followed show the remnants of Hurricane Ivan (2004) becoming engulfed into the eastward moving cold front after recurvature, which led to abundant tornado production, most notably within the mid-Atlantic states. This setup echoes that described by Edwards and Pietrycha (2010) in that tornado outbreaks can occur along baroclinic boundaries given various amounts of shear and buoyancy.

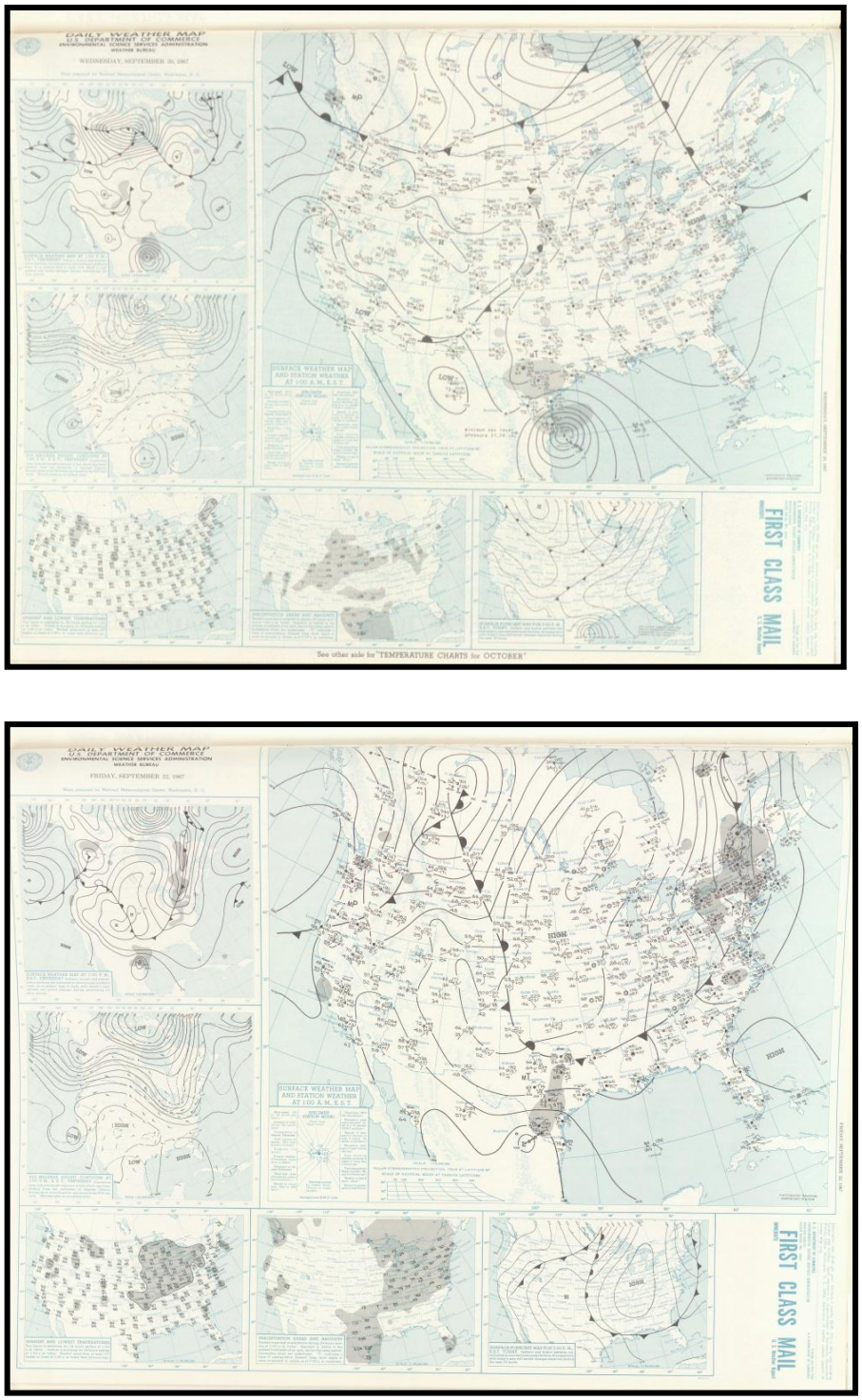

Figure 18: Surface map on day of Beulah's (1967) landfall (top) and two days post- landfall (bottom). Stationary front positioned to the northwest of TC, eventually transitioning to a cold front pressing southwestward.

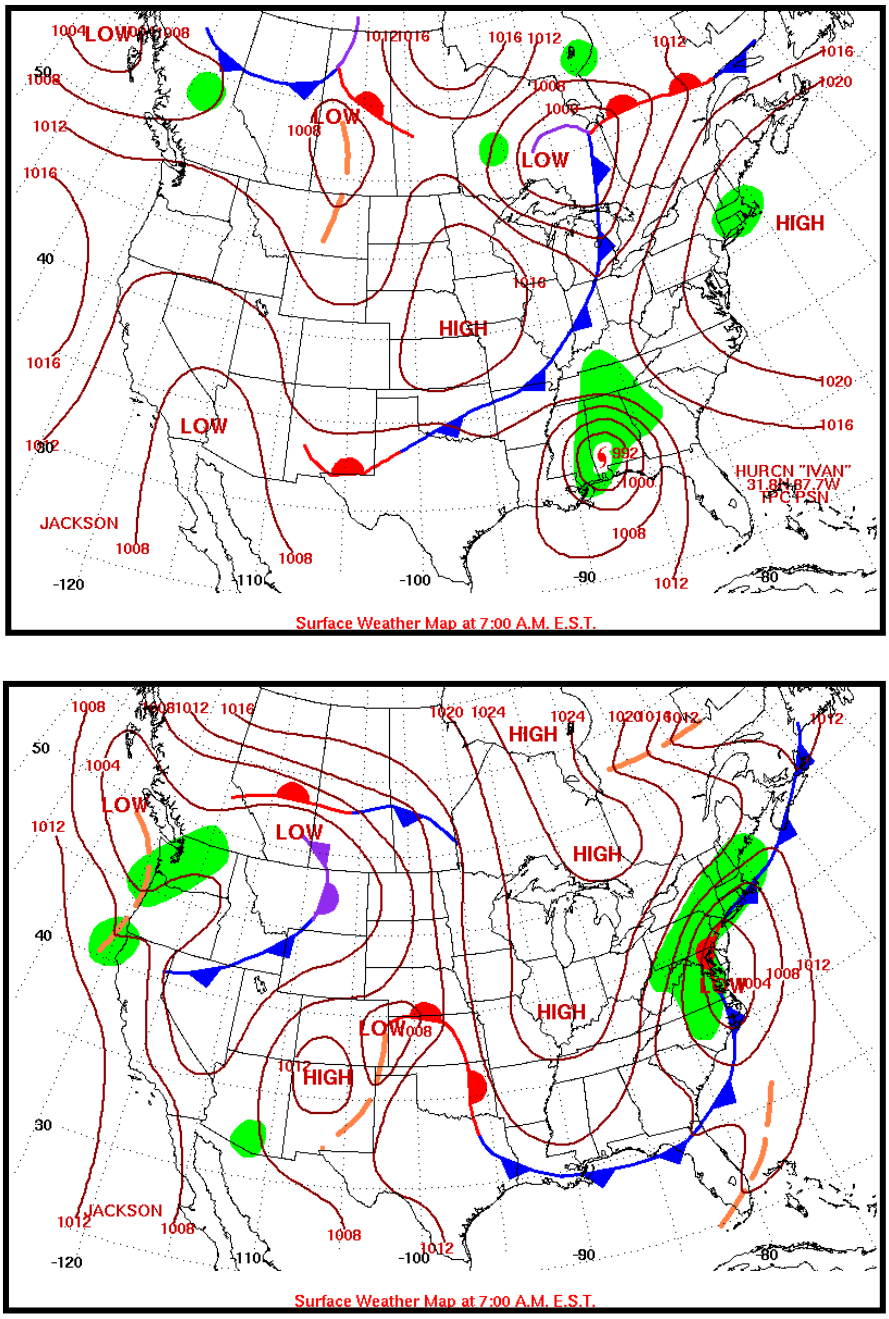

Figure 19: Surface map on date of Ivan's (2004) landfall (top) and two days post-landfall (bottom). A cold front is positioned to the northwest of Ivan's circulation, eventually causing the TC to recurve, with remnants being engulfed into the cold front two days after landfall.

b. Dynamic Analysis

Select dynamic parameters within the 15 TCs of each tornado-producing phase were examined, which were gathered at a time of heightened tornado output. Basic descriptive statistics (each parameter's mean value among the respective phases) were performed, as shown in Figure 20.

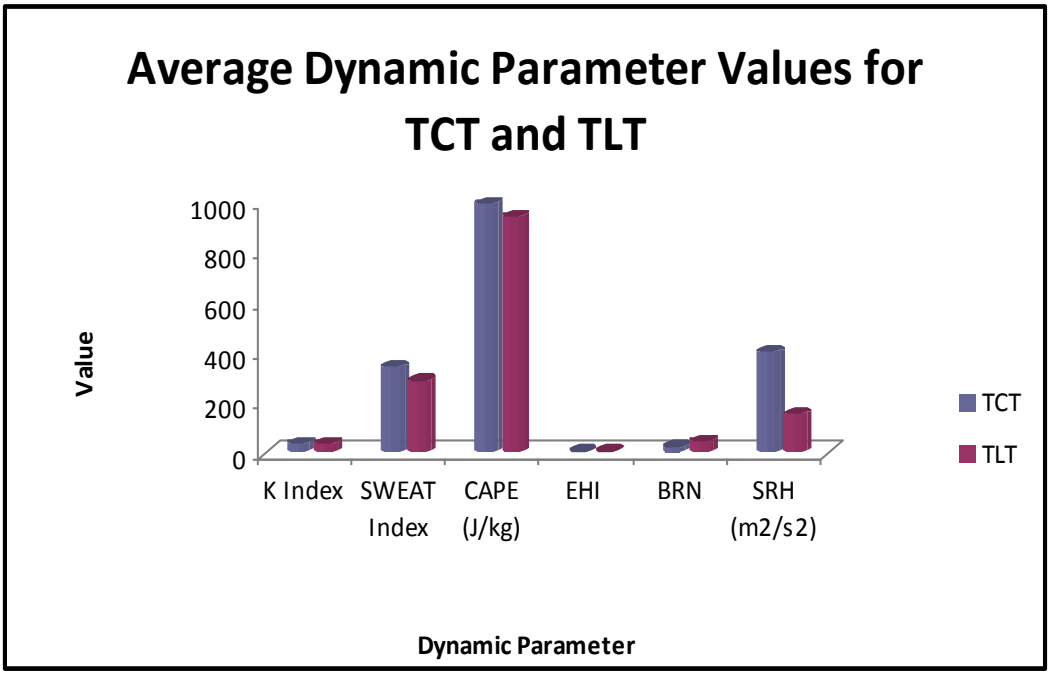

Figure 20: Average dynamic parameter values for TCT and TLT within the sample. Significant results display a higher value of SWEAT, EHI and SRH within the TCT environment than TLT.

It is clear that the majority of parameters within a TCT environment are higher than among the TLT environment as a result of the TC's intensity, given an average tornado output of 45 among the TCT environment and 8 among the TLT environment. When analyzing total parameter values among each storm (Table 8), it is clear that storm-relative helicity values are noticeably higher among TCT intensity storms, displaying greater

amounts of potential rotation within the atmosphere near time of tornado formation, as can be seen in Hurricanes Beulah (1967), Rita (2005), and Ike (2008).

Table 8: Individual values of each parameter among TC phase for all TCs analyzed.

Tropical Cyclone Tornadoes	K Index	Sweat Index	CAPE (J/kg)	EHI	BRN	SRH (m^2/s^2)	Tornado Output
Hurricane Beulah (1967)	35.60	382.40	335.75	1.12	2.96	602.9	117
Hurricane Rita (2005)	33.50	414.83	579.55	2.29	5.01	674.2	104
Hurricane Ivan (2004)	26.80	408.16	2279.13	1.60	61.67	113.1	54
Hurricane Georges (1998)	34.10	284.60	592.41	0.72	12.36	214.7	49
Hurricane Katrina (2005)	40.80	338.00	885.58	2.61	6.49	548.7	49
Hurricane Andrew (1992)	33.30	254.60	526.41	2.47	6.57	565.1	48
Hurricane Gilbert (1988)	38.50	317.80	5256.67	8.14	114.51	264.3	39
Hurricane Allen (1980)	31.90	291.20	629.17	1.25	6.14	376.7	34
Hurricane Ike (2008)	34.60	394.20	524.35	2.62	3.55	824.7	33
Hurricane Danny (1985)	37.80	419.15	1108.01	2.52	10.47	385.5	31
Hurricane Cindy (2005)	23.90	285.10	456.52	0.38	13.79	147.8	28
Hurricane Lili (2002)	34.90	358.59	650.05	1.85	9.91	488.8	27
Hurricane Audrey (1957)	31.40	316.40	37.39	0.11	0.49	299.1	23
Hurricane Alicia (1983)	32.80	275.00	707.63	0.51	22.09	121.7	22
Hurricane Carla (1961)	35.20	350.40	348.76	0.73	3.42	386.5	21

Tropical Low Tornadoes	K Index	Sweat Index	CAPE (J/kg)	EHI	BRN	SRH (m^2/s^2)	Tornado Output
Tropical Storm Fay (2008)	34.90	329.15	2006.37	1.76	35.06	162.7	34
Tropical Storm Bill (2003)	29.10	401.00	168.56	0.27	0.98	298.2	15
Tropical Storm Fay (2002)	40.10	243.80	1634.71	0.48	16.07	7.6	11
Tropical Storm Hermine (2010)	39.10	403.30	2041.63	3.36	27.10	214.9	11
Tropical Storm Chris (1982)	31.50	263.80	692.10	0.62	14.81	124.6	9
Tropical Storm Allison (1989)	33.30	231.80	1684.10	0.58	68.34	53.9	9
Tropical Storm Frances (1998)	38.10	423.35	596.46	0.84	12.63	212.1	9
Tropical Storm Candy (1968)	23.00	392.75	391.81	0.79	6.00	349.6	7
Hurricane Bonnie (1986)	28.10	181.60	2380.25	1.22	316.15	71.5	5
Tropical Storm Debra (1978)	31.20	271.80	109.37	0.06	9.15	62.7	4
Tropical Storm #1 (1964)	33.50	215.40	1289.11	0.65	42.46	79.4	3
Tropical Storm #1 (1960)	25.50	203.00	143.03	0.14	3.00	175.7	3
Tropical Storm Jenny (1969)	30.40	296.60	19.33	0.02	0.28	150.6	2
Tropical Storm Becky (1970)	31.00	219.40	984.66	0.78	64.87	113.3	2
Tropical Storm Beryl (1994)	33.00	229.00	25.93	0.03	0.68	198.8	2

On the basis of shear alone, the dynamic results in Table 8 echo those evaluated among the 850mb chart, showing higher average shear values among TCT than TLT. It can be concluded that tornadoes spawned among the hurricane and tropical storm phases are primarily shear-driven, while CAPE dominates the TLT environment, which is especially evident among Tropical Storms Bonnie (1986), Fay (2008) and Hermine (2010).

The Kolmogorov-Smirnov test shows that all parameters assume a normal distribution (not pictured). Therefore, independent samples t-tests were performed. The results of this test (Table 9) show significance among EHI and SRH, with p-values of .043 and <.01 (alpha level of .05), respectively. While on the border of significance (p-value of .051), the SWEAT index is important and has an impact on potential thunderstorm development and consequent tornado production within a TC environment.

Due to the small sample sizes of only 15 storms in each group, a Mann-Whitney U test was performed in addition to the t tests mentioned above (Table 9). Among the two groups, SWEAT, EHI, and SRH were statistically significant, with p-values of .044, .019, and <.01, respectively. These findings suggest that higher levels of wind shear, and to a lesser extent instability, are imperative in the production of tornadoes within a given TC. Upon individual analysis of the results among these two parameters, EHI values among the TCT environment average twice as high as those of the TLT environment. With EHI resulting from a combination of CAPE and SRH, and SRH playing a statistically significant role in tornado formation, it can be concluded that wind shear is the primary factor in tornado output, regardless of TC phase.

Table 9: Probability values of both Independent Samples t-test and Mann-Whitney U test. Those marked with an asterisk (*) symbol denote significance at the .05 level.

Mann-Whitney U test

K-Index	SWEAT	CAPE	EHI	BRN	SRH
0.198	0.044*	0.917	0.019*	0.373	<.01*

Independent Samples t-test

K-Index	SWEAT	CAPE	EHI	BRN	SRH
0.354	0.051*	0.900	0.043*	0.312	<.01*

*significant at the .05 level

The results of this thesis are not without their limitations, however, as average environmental parameters that were assessed within the synoptic and dynamic environments of Gulf land-falling TCs may not accurately represent each land-falling TC. Furthermore, limited environmental sounding times and locations may not be indicative of the atmosphere at the precise time and location of tornado formation. Likewise, tornadoes associated with East coast land-falling TCs may not imitate the environments presented in this thesis. An analysis of tornadoes associated with these storms would be necessary, which is beyond the scope of this thesis.

5. Conclusion

The purpose of this thesis was two-fold: 1) to determine a possible relationship between TC size, intensity, and tornado output and 2) to analyze intensity differences among two phases of a TC's lifecycle. Relationships between TC intensity and tornado output have been performed within previous literature, however, to the author's knowledge, size was not a factor until the suggestion of McCaul (1991). Until now, no known study has attempted to determine a relationship utilizing all three parameters. Multiple statistical tests were performed in an attempt to determine a relationship between all three parameters, but with little success. It must be noted, however, that, although nonlinear in nature, a relationship exists between TC intensity and tornado output. Moreover, TC size, although not statistically significant, does have a minor influence on tornado output. For the majority of TCs within the period of study, those classified as large in size and 'major' in intensity produced a greater amount of tornadoes.

A secondary goal to this thesis was to examine the characteristics of tornado-producing TCs among two phases of a storm's life cycle; tornadoes within the hurricane and tropical storm phases, termed Tropical Cyclone Tornadoes (TCT) and tropical depression and remnant low-phase tornadoes, defined as Tropical Low Tornadoes (TLT). Assessment utilized both a synoptic and limited dynamic approach, evaluating the average environment at large and small scales. The average characteristics among each tornado-producing phase can be summarized as follows:

TCT environment:

- Synoptic evaluations among various levels display higher wind shear values aiding in uplift and rotation, a pronounced presence of dry air intrusion within the northwest quadrant of land-falling TCs, weakening the TC itself, yet aiding in greater amounts of buoyancy and lift - which enhances tornado potential. The position of a ridge within the Atlantic allows for storm recurvature and greater tornado output, while the alignment of the jet stream north of the Ohio Valley places the right entrance region of the embedded jet max within the vicinity of TCs, allowing for increased uplift and divergence, intensifying the potential for tornadoes to occur.

- The dynamic parameters associated with TCT echo the average synoptic patterns described above. On average, CAPE values remain positive, displaying signs of instability within the surrounding environment. Storm-relative helicity is very high, conducive of a shear-dominated atmosphere, favorable for rotation. The EHI resonates these average values, which are supportive of supercell development and tornadic potential. Furthermore, supercell development within this phase of a TC life cycle is imminent, with moderate convective potential surrounding an atmosphere capable of producing a great amount of severe weather, including potential tornado outbreaks.

TLT environment:

- Smaller average values of low-level wind shear coupled with a broad area of RH may partially explain the lack of tornado output among dissipating TCs in the study area. While a substantial amount of tornadoes have been shown to spawn in the region of

divergence to the right of a trough axis, the 200mb jet maxes are displaced, prohibiting the divergence necessary to spawn additional tornadoes.

- Similar to the TCT environment, an equal amount of instability is present among the TLT environment, yet, among individual assessment of the 15 TCs in study, it is determined that high levels of CAPE remain the driving force, with average BRN values higher than that of TCT. With this setup, strong updrafts are possible within this environment, but shear values necessary for rotation remain weak on average, which may shed light on the smaller amount of tornadoes among this phase. Furthermore, SRH and EHI values show a much smaller average than what is found within hurricane and tropical storm tornadoes, yet these values still support tornado development.

These results are beneficial to operational forecasters and climatologists alike and serve as an enhancement to traditional forecasting of tornadoes associated with land-falling TCs. By understanding the contributing factors and characteristics associated with TCs of various size and intensity parameters, better forecasting can be generated and the public alerted so that proper plans can be executed.

References

Agee E.M., & Hendricks, A. (2011). An assessment of the climatology of Florida hurricane-induced tornadoes (HITs): technology versus meteorology. *Journal of Climate*, 24, 5218–5222.

Baker, A.K., Parker M.D. &Eastin, M.D. (2009). Environmental ingredients for supercell and tornadoes within Hurricane Ivan. *Weather and Forecasting*, 24, 223-244.

Belanger, J.I, Curry, J.A., & Hoyos, C.D. (2009). Variability in tornado frequency associated with U.S. landfalling tropical cyclones. *Geophysical Research Letters*, 36, L17805.

Blake, E.S., Landsea, C.W., & Gibney, E.J. (2011). The deadliest, costliest, and most intense United States tropical cyclones from 1851 to 2010 (and other frequently requested hurricane facts). *NOAA Technical Memorandum NWS NHC-6*. National Weather Service, National Hurricane Center, Miami, FL. [Available online at http://www.srh.noaa.gov/www/images/tbw/1921/DeadliestHurricanes.pdf].

Cecil, D.J., & Schultz, L.A. (2010). Tropical cyclone tornadoes: synoptic scale influences and forecasting applications. Preprints, 29th Conference on Hurricanes and Tropical Meteorology, Tucson, AZ, American Meteorological Society, 1C.4 [Available online at http://ams.confex.com/ams/29Hurricanes/techprogram/paper_168674.htm].

Cohen, A.E. (2010). Synoptic-scale analysis of tornado-producing tropical cyclones along the Gulf coast. *National Weather Digest*, 34 (2), 99-115.

CSC [Coastal Services Center]. 2011. Historical Hurricane Tracks. Charleston, S.C.: National Oceanic and Atmospheric Administration, Coastal Services Center. [http://csc.noaa.gov/hurricanes/#].

Curtis, L. (2004). Midlevel dry intrusions as a factor in tornado outbreaks associated with landfalling tropical cyclones form the Atlantic and Gulf of Mexico. Weather Forecasting, 19, 411-427.

Davies, J.M. (2006). Hurricane and tropical cyclone tornado environments from RUC proximity soundings. Preprints, 23rd Conference on Severe Local Storms, St. Louis, MO, American Meteorological Society, P8.1 [Available online at http://ams.confex.com/ams/23SLS/techprogram/paper_115483.htm].

Davies-Jones, R. (1984). Streamwise vorticity: The origin of updraft rotation in supercell storms. *Journal of Atmospheric Sciences*, 41, 2991-3006.

Eastin, M.D., & Link, M.C. (2009). Miniature supercells in an offshore outer rainband of Hurricane Ivan (2004). *Monthly Weather Review*, 137, 2081-2104.

Edwards, R. (2008). Tropical cyclone tornadoes – a research and forecasting overview. Part 1: Climatologies, distribution, and forecast concepts. Preprints, *24th Conference on Severe Local Storms*, Savannah, GA, American Meteorological Society, 7.A.1 [Available online at http://ams.confex.com/ams/24SLS/techprogram/paper_141721.htm].

Edwards, R. (2010). Tropical Cyclone tornado records for the modernized NWS era. Preprints, *25th Conference on Severe Local Storms*, Denver, CO, American Meteorological Society, P3.1 [Available online at http://ams.confex.com/ams/25SLS/techprogram/paper_175269.htm].

Edwards, R. & Pietrycha, A.E. (2006). Archetypes for surface baroclinic boundaries influencing tropical cyclone tornado occurrence. Preprints, *23rd Conference on Severe Local Storms*, St. Louis, MO, American Meteorological Society, P8.2 [Available online at http://ams.confex.com/ams/23SLS/techprogram/paper_114992.htm].

Edwards, R., Dean, A.R., Thompson, R.L., & Smith, B.T. (2010). Objective environmental analyses and convective modes for U.S. tropical cyclone tornadoes from 2003-2008. Preprints, *25th Conference on Severe and Local Storms*, Denver, CO, American Meteorological Society, P3.2 [Available online at http://ams.confex.com/ams/25SLS/techprogram/paper_175397.htm].

Gentry, R.C. (1983). Genesis of tornadoes associated with hurricanes. *Monthly Weather Review*, 111, 1793-1805.

Hagemeyer, B.C. (1997). Peninsular Florida tornado outbreaks. *Weather Forecasting*, 12, 399-427.

Hagemeyer, B.C. (1998). Significant tornado events associated with tropical and hybrid cyclones in Florida. Preprints, *16th Conference on Weather Analysis and Forecasting*, Phoenix, AZ, American Meteorological Society, 4-6.

Hagemeyer, B.C. & Hodanish, S.J. (1995). Florida tornado outbreaks associated with tropical cyclones. Preprints, *21st Conference on Hurricanes and Tropical Meteorology*, Miami, FL, American Meteorological Society, 312-314.

Hill, E.W., Malkin, J.W., & Schulz, A. (1966). Tornadoes associated with cyclones of tropical origin-practical features. *Journal of Applied Meteorology*, 5, 745-763.

IBM Corporation (2012). *SPSS Statistical Software: Version 19*. Armonk, NY

Jarvinen, B.R., Neumann, C.J., & Davis, M.A.S. (1984). A tropical cyclone data tape for the North Atlantic basin, 1886-1983: Contents, limitations, and uses, NOAA Technical Memorandum NWS NHC 22 (1984).

Kalnay, E. (1996). The NCEP/NCAR reanalysis 40-year project. *Bulletin of the American Meteorological Society*, *77*, 437-471.

Kimball, S. K., & Mulekar, M. S. (2004). A 15-year climatology of North Atlantic tropical cyclones. Part I: Size parameters. *Journal of Climate*, *2004*, 3555-3575.

Landsea, C. W., Anderson, C., Charles, N. Clark, G., Dunion, J., Fernandez-Partagas, J., Hungerford, P., Neumann, C., & Zimmer, M. (2004). The Atlantic hurricane database reanalysis project: Documentation for 1851 – 1910 alterations and additions to HURDAT database, in *Hurricanes and Typhoons: Past, Present and Future*, R.J. Murnane and K.B. Liu, Eds., 177– 221. Columbia University Press, New York. [Available online at http://www.aoml.noaa.gov/hrd/Landsea/rpibook-final04.pdf].

Latour, M.H., & Bunting, D.C. (1949). Radar observation of a Florida hurricane, August 26-27, 1949. *Bulletin No. 29*, University of Florida, Engineering and Industrial Experiment Station, Oct. 1949.

Maddox, R.A. (1973). A study of tornado proximity data and an observationally derived model of tornado genesis. *Atmospheric Science Report No. 212*. Colorado State University, Fort Collins, CO. 101pp.

Malkin, W. & Galway, J.G. (1953). Tornadoes associated with hurricanes as illustrated by Franconia, VA, tornado, September 1, 1952. *Monthly Weather Review*, 81, 299-303.

McCaul, E.W. (1987). Observations of the Hurricane "Danny" tornado outbreak of 16 August 1985. *Monthly Weather Review*, 115, 1206-1223.

McCaul, E.W. (1991). Buoyancy and shear characteristics of hurricane-tornado environments. *Monthly Weather Review*, 119, 1954-1978.

McCaul, E.W., & Weisman, M.L. (1996). Simulations of shallow supercell storms in landfalling hurricane environments. *Monthly Weather Review*, 124, 408-429.

Moore, T.W., & Dixon, R.W. (2011). Climatology of tornadoes associated with Gulf coast land-falling hurricanes. *The Geographical Review*, 101 (3), 371-395.

Moore, T.W., & Dixon, R.W. (2012).Tropical cyclone-tornado casualities. *Natural Hazards*, 61 (2), 621-634.

NCDC [National Climatic Data Center]. 2011. Storm Event Database. Asheville, N.C. National Oceanic and Atmospheric Administration, National Environmental Satellite, Data, and Information Service, National Climatic Data Center. [http://www4.ncdc.noaa.gov/cgi-win/wwcgi.dll?wwEvent~Storms].

NHC [National Hurricane Center]. 2011. NHC Archive of Hurricane Seasons: Hurricane Season Tropical Cyclone Report. Miami, FL: National Oceanic and Atmospheric Administration, National Weather Service, National Hurricane Center. [http://www.nhc.noaa.gov/pastall.shtml].

NHC [National Hurricane Center]. 2012. The Saffir-Simpson Hurricane Wind Scale. Miami, FL: National Oceanic and Atmospheric Administration, National Weather Service, National Hurricane Center. [http://www.nhc.noaa.gov/sshws.shtml].

NOAA [National Oceanic and Atmospheric Administration]. (2007). NOAA Central Library Data Imaging Project, Daily U.S. Weather Maps Project. Accessed 23 May 2012. [Available online at http://docs.lib.noaa.gov/rescue/dwm/data_rescue_daily_weather_maps.html].

NOAA [National Oceanic and Atmospheric Administration]. 2012. Atlantic Hurricane Research Division. U.S. Department of Commerce. [http://www.aoml.noaa.gov/hrd/hurdat/easyread-2012.html].

Novlan, D., & Gray, W. (1974). Hurricane-spawned tornadoes. *Monthly Weather Review*, 102, 476-488.

NWS [National Weather Service].Weather Forecasting Office, Louisville, KY. (2004). Convective Seasonal and Environmental Parameters and Indices. Accessed 14 June 2012. [Available online at http://www.crh.noaa.gov/lmk/soo/docu/indices.php].

Orton, R. (1970). Tornadoes associated with hurricane Beulah on September 19-23, 1967. *Monthly Weather Review*, 98, 541-547.

Pearson, A., & Sadowski, A. (1965). Hurricane-induced tornadoes and their distribution. *Monthly Weather Review*, 93, 461-464.

Pielke, R.A. Simonpietri, C. & Oxelson, J. (1999).Thirty Years After Hurricane Camille: Lessons Learned, Lessons Lost. University of Colorado. Accessed 5 April 2012.

Plymouth State Weather Center RAOB Selector for Archived CONUS Data. Plymouth State University. Web. Accessed 3 February 2012.

Rao, G.V., Scheck, J.W., Edwards, R., & Schaefer, J.T. (2005). Structures of mesocirculations producing tornadoes associated with Tropical Cyclone Francis (1998). *Pure and Applied Geophysics*, 162, 1627-1641.

Rappaport, E.N. (1993). Hurricane Andrew Preliminary Report. National Hurricane Center. [Available online at http://www.nhc.noaa.gov/1992andrew.html].

Rappaport, E. N. (2000). Loss of life in the United States associated with recent Atlantic tropical cyclones. *Bulletin of the American Meteorological Society, 81*, 2065-2073.

Rauber, R.M., Walsh, J.E., & Charlevoix, D.J. (2008). *Severe and Hazardous Weather: An Introduction to High Impact Meteorology, Third Edition*. Kendall/Hunt Publishing Company.

Sadowski, A. (1962). Tornadoes associated with hurricane Carla, 1961. *Monthly Weather Review*, 90, 514-516.

Schneider, D. & Sharp, S. (2007). Radar signatures of tropical cyclone tornadoes in central North Carolina. *Weather Forecasting*, 22, 278-286.

Schultz, L.A. & Cecil, D.J. (2009). Tropical Cyclone Tornadoes, 1950-2007. *Monthly Weather Review*, 137, 3471-3484.

Showalter, A.K., & Fulks, J.R. (1943). *Preliminary Report on Tornadoes*, U.S. Weather Bureau, Washington, D.C.

Smith, J.S. (1965). The hurricane-tornado. *Monthly Weather Review*, 93, 453-459.

Spratt, S.M., Sharp, D.W., Welsh, P., Sandrik, A., Alsheimer, F. & Paxton, C. (1997). A WSR-88D assessment of tropical cyclone outer rainband tornadoes. *Weather Forecasting*, 12, 479-501.

SPC [Storm Predication Center]. N.d. Fujita Tornado Damage Scale. Norman, OK: National Oceanic and Atmospheric Administration, National Weather Service, Storm Predication Center. [http://www.spc.noaa.gov/faq/tornado/ef-scale.html].

Tepper, M. (1950). Radar and synoptic analysis of a tornado situation. *Monthly Weather Review*, 78 (9), 170-176.

Tepper, M. (1950). On the origin of tornadoes. *Bulletin of the American Meteorological Society*, 31 (9), 311-314.

Vasquez, T. (2003). *Weather Map Handbook: a guide to the Internet, modern forecasting, and weather technology*. Weather Graphics Technologies.

Verbout, S.M., Schultz, D., Leslie, L., Brooks, H., Karoly, D. & Elmore, K. (2007). Tornado outbreaks associated with landfalling hurricanes in the Atlantic basin: 1954-2004. *Meteorology & Atmospheric Physics*, 97, 255-271.

Weiss, S. (1985). On the operational forecasting of tornadoes associated with tropical cyclones. Preprints, *14th Conference on Severe Local Storms*, Indianapolis, IN, American Meteorological Society, 293-296.

Willis, T. (1969). Characteristics of the tornado environment as deduced from proximity soundings. Preprints, *6th Conference on Severe Local Storms*, Chicago, IL, American Meteorological Society, 222-229.

Appendix A – Convective Parameters and Indices (extracted from the National Weather Service Weather Forecast Office, Louisville, KY.

http://www.crh.noaa.gov/lmk/soo/docu/indices.php)

K Index

K below 30:	Thunderstorms with heavy rain or severe weather possible (see note below).
K over 30:	Better potential for thunderstorms with heavy rain.
K = 40:	Best potential for thunderstorms with very heavy rain.

SWEAT Index

SWEAT over 300:	Potential for severe thunderstorms.
SWEAT over 400:	Potential for tornadoes.

CAPE

CAPE below 0:	Stable.
CAPE = 0 to 1000:	Marginally unstable.
CAPE = 1000 to 2500:	Moderately unstable.
CAPE = 2500 to 3500:	Very unstable.
CAPE above 3500-4000:	Extremely unstable.

EHI

EHI below 1.0:	Supercells and tornadoes unlikely in most cases, but be aware of convective interactions and shear zones that could make EHI values unrepresentative.
EHI = 1.0 to 2.0:	Supercells and tornadoes are possible but usually tornadoes are not of violent or long-lived. Can get non-supercell/shear vorticy tornadoes near the leading edge of bow echoes/LEWPS.
EHI = 2.0 to 2.4:	Supercells more likely and mesocyclone-induced tornadoes possible.
EHI = 2.5 to 2.9:	Mesocyclone-induced supercellular tornadoes more likely.
EHI = 3.0 to 3.9:	Strong mesocyclone-induced tornadoes (F2 and F3) possible.
EHI over 4.0:	Violent mesocyclone-induced tornadoes (F4 and F5) possible.

BRN

BRN below 10:	Strong vertical wind shear and weak CAPE. The shear may be too strong given the weak buoyancy to develop sustained convective updrafts. However, given sufficient forcing, thunderstorms may still develop; if so, rotating supercells could evolve given the high shear.
BRN =10 to 45:	Associated with supercell development.
BRN over 50:	Relatively weak vertical wind shear and high CAPE which suggests multicellular thunderstorm development is most likely.

SRH

Hs-r = 150:	The approximate threshold for supercell development.
Hs-r = 150 to 299:	Weak tornadoes (F0 and F1) possible.
Hs-r = 300 to 449:	Strong tornadoes (F2 and F3) possible.
Hs-r over 450:	Violent tornadoes (F4 and F5) possible.